J Mater Sci: Mater Electron (2020) 31:21856–21895

Review

Development of polymeric active layer for RGB light-emitting devices: a review

Elisa Barbosa de Brito[1], Rogerio Valaski[2], and Maria de Fátima Vieira Marques[1,*]

[1] *Instituto de Macromoleculas Professora Eloisa Mano, IMA, Universidade Federal do Rio de Janeiro, IMA- UFRJ, Av. Horacio Macedo 2030, Rio de Janeiro, RJ 21941-598, Brazil*

[2] *Instituto Nacional de Metrologia, Qualidade e Tecnologia (Inmetro), Xerém, Brazil*

Received: 6 July 2020
Accepted: 1 November 2020
Published online: 13 November 2020

ABSTRACT

Due to the demand for materials that have promising properties for the electronic device market, the development of new conjugated polymers, where the π bond is responsible for the material's optoelectronic properties, has attracted the attention of the academic and industrial community owing to the easy processability, which can be performed from a polymeric solution, and to a great potential for the manufacture of devices such as cell phone screens, televisions, light-emitting diodes, and solid-state lighting (SSL). For SSL applications, usually, polymers capable of emitting red, green, and blue (RGB) light bands are used, which combined, generate white light. Thus, this review presents some of the most relevant works that aim at developing RGB devices that can be used for SSL applications.

1 Introduction

The impressive evolution in the synthesis of organic compounds led to the emergence of a promising research line, organic electronics (EO). This area stands out for promoting research in the production and development of electronic devices based on organic semiconductors. The development of organic semiconductors began in the late 1990s. Its discovery led to the awarding of researchers Alan J. Heeger, Alan G. MacDiarmid, and Hideki Shirakawa to the Nobel Prize in Chemistry in 2000 [1, 2].

Organic semiconductors are made up of conjugated organic molecules and are chemically manipulable materials that exhibit technological interesting electrical and optical properties. The main advantages of this type of material, especially polymeric over inorganic semiconductors, are its low production cost, low density, malleability, flexibility, and ease of forming polymer films [3, 4].

The polymeric semiconductors can be considered electron (n-type semiconductor) or hole (*p*-type semiconductor) carriers. However, they do not have a well-organized crystal structure. In general, polymer semiconductors have a large number of crystal defects, resulting from their long molecular chains, creating energy traps in the chemical structure. These defects in the structure may also be caused by the

Address correspondence to E-mail: fmarques@ima.ufrj.br

https://doi.org/10.1007/s10854-020-04809-2

degradation process or the development of supramolecular structures [5, 6].

Based on the distribution of these defects in polymer materials, the transport of charges is limited by energy states. Thus, the transport occurs through a hopping mechanism, in which the charge carriers (electron or hole) move across well-defined energy states through jumps. These energy states constitute the molecular energy orbitals, where the valence band in inorganic semiconductors corresponds to the energy level of the highest occupied molecular orbital (HOMO). In contrast, the conduction band is equivalent to the lowest unoccupied molecular orbital (LUMO) energy. Holes are transported by HOMO, whereas electrons are transported by LUMO so that the energy difference between orbitals is the bandgap [7, 8].

The great diversity of these conjugated polymer molecules and the possibility of modifications through synthesis helps the continuous search for miniaturization of electronic devices, promoting the renewal of current technologies and making this area a possible substitute for conventional electronics, with the development of less thickness, although larger area, flexible, and resistant devices [9–11].

Known applications for such semiconductors include light-emitting organic diodes (OLEDs), which are devices that, when subjected to an electric field, whether intense or not, have the property of emitting light [12]. Such devices can be classified as Small Organic Light Emitting Diode (SMOLED), designed by low molecular weight organic molecules, which are usually combined with π type connections, and the Organic Polymer Light Emitting Diode (PLED), which will be reported in the present work. PLED consists of polymers that have a succession of single (σ) and double bonds. The π bond is responsible for the properties of these materials for optoelectronic use and, thus, it can conduct electrical impulses with unpaired electrons delocalized throughout the polymeric structure [4, 13, 14].

At the moment, a very small number of conjugated polymers of type n are reported, compared to type p. Thus, studies on the development and strategies for designing n-type polymers are carried out. Most of the conjugated polymers are dependent on the π bond that alternate in the polymer main chain; another strategy formulated is the alternation of the p-π conjugation, in which the p orbitals of the heteroatoms conjugate with the π orbitals of the units in the main chain thus, opportunities to adjust the electronic structure of the conjugated polymers [15–17].

The study of polymer-emitting devices began in 1990, with Burroughes and colleagues, following the research by Tang and VanSlyke in 1987 on multilayer organic small-molecule emitting devices. They began to develop a device consisting of poly(*p*-phenylene vinylene) (PPV), this being the component of the first commercial PLED [18]. Another commonly used polymer is poly (9-vinylcarbazole) (PVK), an unconjugated polymer with good thermal and chemical stability and is soluble in various solvents, such as benzene, toluene, chloroform, and tetrahydrofuran. This polymer acts as a means of transporting holes and is coated by rotation, which is essential for this processing [19, 20]. However, its use in electronic devices is not in pure form but in mixtures with coordination compounds or functionalization to improve their electrical and conduction properties [21, 22]. For presenting such properties, it has been reported as a buffer layer, playing an important role in the process of energy transfer between the host material and the dopant since it has been shown that PVK has good chemical compatibility and high triplet energy for the polymeric guest/host mixture [23, 24].

The expansion and development of this technology have impacted the reduction of operating voltage, resulting in greater efficiency of these devices. However, other parameters beyond composition influence the best performance of the material, which are the morphology of the deposited polymeric film, as well as the thickness of this layer. Thus, attention should be paid to the polymer's appropriate solvent and the appropriate deposition technique [25–30].

The difficulties in producing these devices are related to the degradation that occurs when they are subjected to electric fields in the presence of oxygen or light because, as mentioned by many authors [31–34], oxygen acts on breaking the polymer chain or interrupting conjugation by replacing groups C=C with C=O. Thus, the devices are sensitive to oxygen and moisture. They require encapsulation in an inert atmosphere, an expensive process [35].

Therefore, it is necessary to develop strategies in its construction so that the PLED device has durability combined with ideal performance. Thus, a systematic study of conjugated polymers' optical and electronic properties is necessary to improve PLED devices' manufacture. However, light emission from

polymeric devices is currently lower than in inorganic materials (LED); therefore, intensive studies are being conducted to improve their performance. The main advantage of PLEDs is the ease of processing since the polymer shows dissolubility in usual organic solvents, forming solid films of nanometric thickness under a substrate or adjacent layers that configure the device [25, 36–39].

2 Polymer light-emitting diodes (PLED)

PLEDs are made up of conjugated polymers that follow the principle of electroluminescence, i.e., when a voltage is supplied through an electric current in the PLED, it emits light [28] (Fig. 1). These diodes have been the subject of intense research due to their superior properties of high efficiency and their great potential in solid-state lighting (SSL) and display applications. The polymers used in these devices have some advantages, such as low manufacturing cost, the possibility of production in large substrate areas of the substrate, and better controllable doping concentrations [40–43].

Thus, thin-film deposition techniques with an optimized sequence of organic semiconductors (OSCs) are employed, where each layer performs a function for the best light emission performance. The deposition of these layers can be performed with low-cost production techniques on large substrates. Thus, it is possible to manufacture devices that emit in a large area, which makes them suitable for diffuse lighting [44–46].

Light-emitting polymers (LEPs) can have their structure fully conjugated, including those with conjugated segments in the structure or side groups, or not conjugated [47–49]. This must-have high quantum photoluminescence efficiency, thermal and chemical stability, good processability, and color purity. The color emitted by such polymers depends on their chemical composition, the nature of the side groups, and the energy difference between the HOMO and LUMO molecular orbitals of the emitting organic material [50, 51].

Among the families of polymers commonly used in the manufacture of light-emitting devices are polycarbazoles, polyphenylenes, polyfluorenes, and polythiophenes. However, another class of polymers has been gaining prominence. These polyfluorene derivatives exhibit efficient electroluminescence linked to a high charge carrier mobility, besides good processability and excellent thermal and chemical stability [52–54].

However, a problem commonly encountered in multilayer devices is the dissolution of the polymer layer by the solution of the subsequent layer, as well as the large bandgap and poor mobility of charge carriers. Thus, composites with coordinating compounds have been developed, forming a guest/host compound, a strategy to improve the diode performance since both materials' properties are combined [55, 56]. This approach was developed in the work of Zanoni and Ilha [57, 58]. They elaborated an OLED device with sky-blue color emission, where the active layer was composed by PVK and a complex of [Ir(Fppy)$_2$(Mepic)], where Fppy = 2-(2,4-difluorophenyl)pyridinate; Mepic = 3-methyl pyridine-2-carboxylate), designed by molecular engineering to optimize the most efficient blue color emission [40]. The built device had the following configuration, FTO/PEDOT:PSS/PVK:FIrMepic, (10% m/m)/Al, where PEDOT:PSS is the mixture of poly(3,4-ethylenedioxythiophene) with poly(styrenesulfonate). The best performance was achieved by modifying the active layer by inserting the iridium complex into the polymer, resulting in higher efficiency associated with energy transfer from the polymer to the complex, a desired feature in OLEDs

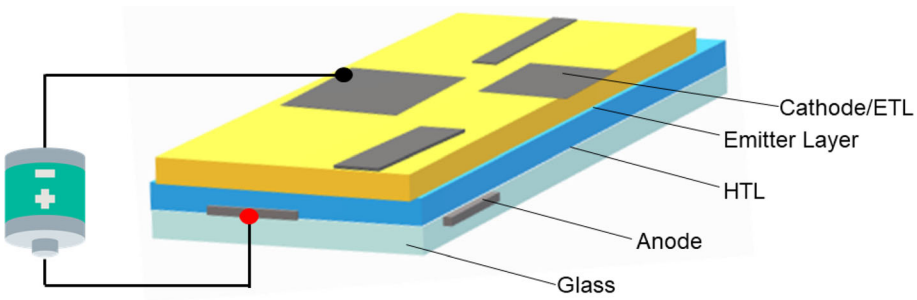

Fig. 1 General schematic representation of a PLED device

as it is a strategy for the extraction of the singlet and triplet generated excitons [59].

An alternative to optimize the injection balancing of holes and electrons in the device is the development of copolymers and/or polymer doping, which reveals improved emission efficiency [53]. The transport of the carriers (hole and electron) is commonly unbalanced because the mobility of the hole is greater than that of electrons, thus affecting electroluminescent efficiency as well as the elaborated device is more susceptible to degradation [60, 61].

Such a method is employed in the research of Ahmad [62], when he developed a PPV copolymer, specifically poly[(4,6)-dimethyl)-1,3-phenylene vinylene-3-methoxy-1,4-phenylene-1,10-dioxydecamethylene-2-methoxy-1,4-phenylene) (Fig. 2).

Conductive polymers such as PPV are promising materials in the field of electronic devices because they are versatile and easy to produce. However, their rigid structure results in low solubility associated with high dielectric incompatibility with conventional solvents [63–66]. An alternative to overcome this problem is to introduce unconjugated flexible spacers in the polymer backbone. It was the strategy developed by Ahmad [62] when he inserts extensors of the unconjugated chain between the aromatic rings in the PPV chain.

2.1 Device constituents

Over the years, the device architectures have become more complex, as shown in Fig. 3. The OLED device can have numerous layers, the first being the substrate where the subsequent layers will be deposited, allowing light to pass through. Usually, polyethylene terephthalate (PET) film or glass is employed. The anode, a conductive transparent oxide (TCO), has the function of efficiently injecting positive charges (holes) into subsequent organic layers and typically employs tin-doped indium oxide (ITO) or fluorine-doped tin oxide (FTO).

Then, the functional layers are deposited; some of them are described in Fig. 4, which is the hole injection layer (HIL), hole transport layer (HTL), electron blocking layer (EBL), emission layer (EML) (or active layer), hole blocking layer (HBL), electron transport layer (ETL), and electron injection layer (EIL) [51, 67, 68].

In the hole injection layer, materials with high charge mobility, high glass transition temperature, and electron blocking capacity are normally employed. The insertion of this layer assists in reducing the energy barrier to inject holes into the device. Examples of materials used for such a function are copper (II) phthalocyanine (CuPc) and 4,4′,4′′-tris[phenyl(*m*-tolyl)amino]triphenylamine (m-MTDATA), as they have a HOMO level comparable to ITO anode work function [69–71].

The electron-blocking and hole blocking layers (EBL and HBL, respectively) are employed when it is necessary to confine the charge carriers to the emitting layer and to separate the HTL and ETL layers from the emitting layer, whenever they contain

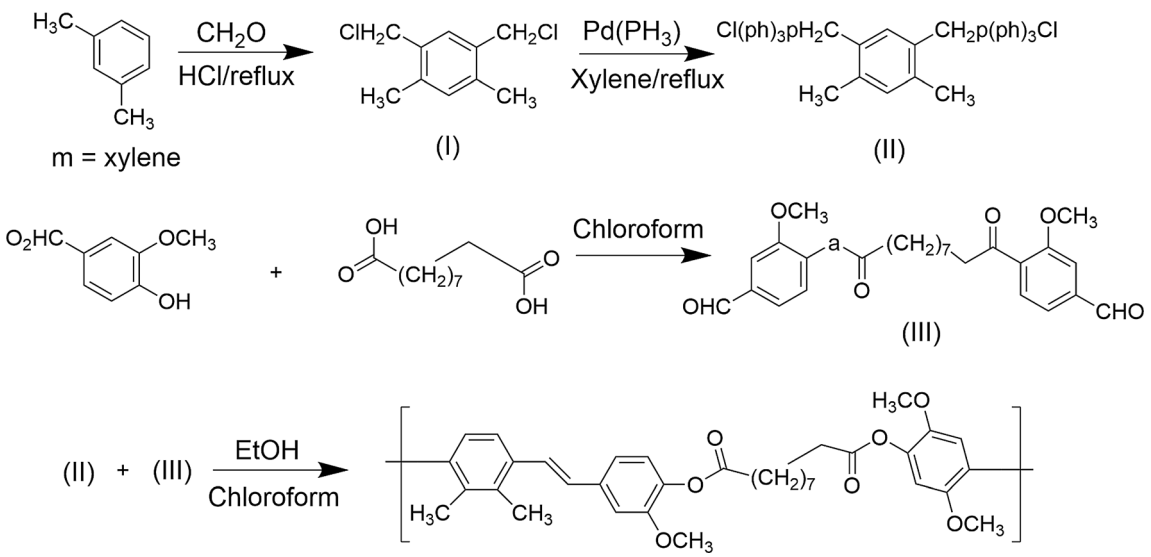

Fig. 2 PPV copolymer synthesis route

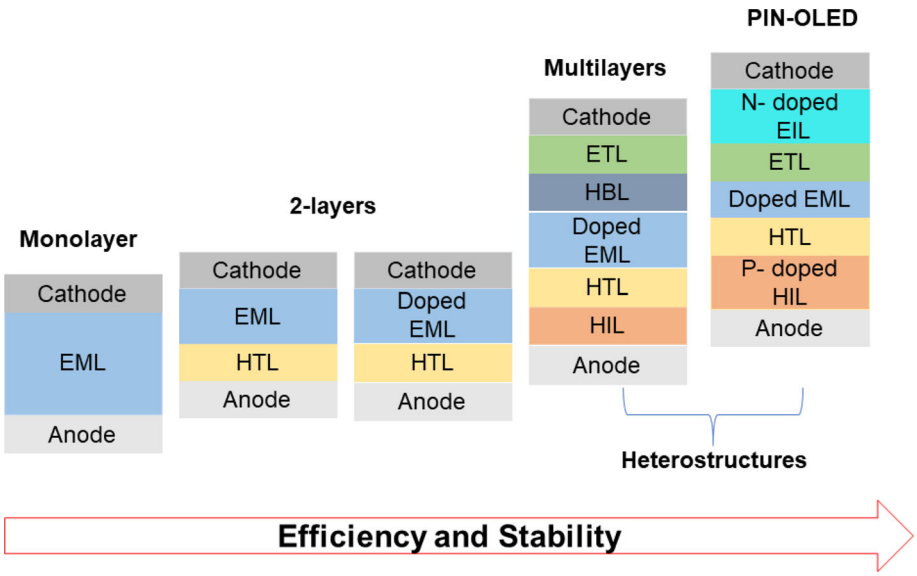

Fig. 3 Evolution of OLED architectures

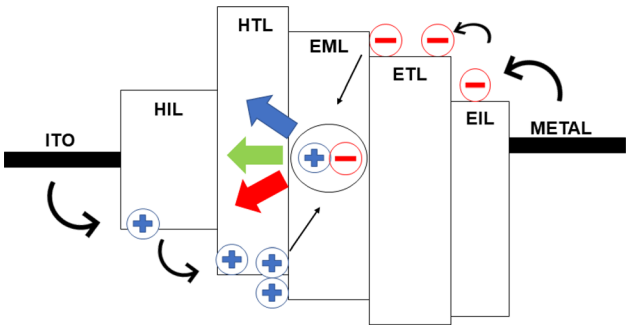

Fig. 4 Constituent layers of an OLED device

doping substances excitonic losses for representing effective quenching sites [72, 73]. The hole-carrying layer (HTL) in the conventional architecture is usually made up of a mixture of semiconductor polymers such as PEDOT:PSS, one of the most efficient materials due to excellent film-like conductivity, solubility, air stability, and optical characteristics (high visible region transparency). The conductive transparent oxide (TCO) layer functions to transport the positive charge to the emitting layer; it also works as an optical spacer to maximize light decoupling. The materials employed for this function usually have low ionization potential and high hole mobility [74].

The active layer (EML) in PLED devices consists of an electroluminescent polymer that is often diluted in an appropriate solvent. The material used as emitting polymer must have a high glass transition temperature so that the elaborate device has a long service life, high emission efficiency, and color purity. This layer has the device's central function since it is where the charges are recombined with subsequent light emission. The polymers used are dependent on the required color since they can be chosen according to the energy difference between the HOMO and LUMO molecular orbitals (bandgap), so the energy released during charge recombination is within the desired wavelength range. Over this layer is deposited EIL, which improves the transport of electrons to the active layer. Due to the required high energy level of HOMO, few materials can be used, but these must have high electronic affinities as well as high ionization potentials. Examples of materials employed for such a function are 8-hydroxyquinolinolate lithium (Liq) and 2,9-dimethyl-4,7-diphenyl-1,10-phenanthroline (BCP), lithium fluoride (LiF) and tris(8-hydroxyquinolinate)) aluminum (Alq_3) [75, 76].

The electron injector layer (EIL), in turn, is a layer that reduces the potential barrier in order to increase the electron density inside the polymer. The materials employed must meet high load mobility requirements, high glass transition temperature, and the ability to block holes [77].

Finally, a metal layer is added, acting as the device's cathode and injecting the electrons. In general terms, aluminum (Al), magnesium (Mg), or calcium (Ca) are used in this layer, as these metals have low ionization potential [38, 72].

2.2 Functional principle

The principle of operation of light-emitting organic diodes is based on the recombination of excitons, i.e.,

the junction of charge carriers (holes and electrons). This process is summarized in five steps, presented in Fig. 5. These are: (1) applying an external voltage through the electrodes, where the holes are injected in the anode, which usually consists of a thin film of ITO, and the electrons in the cathode, from a low work function metal contact; (2) transport of charge carriers to the active layer at the site of recombination, whereby thin electron-blocking layers and holes can be added to the device structure to aid selective charge transport and prevent non-radioactive recombination. The displacement of the holes is through the HOMO molecular orbitals of this layer. At the same time, the electrons are transported by the electron transport layer (ETL), where the transport occurs through the LUMO molecular orbitals of this layer.

(3) The charge carriers migrate through the layers constituting the device and recombine into the active layer, known as the recombination zone, which gives rise to a near-particle neutral bound state called the exciton. Energy barriers for electrons and holes around the emitting layer help in the confinement of these carriers and, consequently, improve the recombination process; (4) there is, therefore, the diffusion of the exciton by about 20 nm and after that, (5) the decay, in which the excitation energy from the excitons can be transferred to the excited singlet and triplet states of the molecular electroluminescent compound (EL). Light is produced in most organic compounds by the rapid decay of the compound's singlet excited molecular states. The color emitted depends on the energy difference (bandgap) between these states and the ground state of compound EL.

Part of the energy is usually lost by the non-radioactive decay of the excited triplet states of the exciton triplet energy transfer. However, much research has been continuously conducted so that this energy from the trigeminal state can also be harnessed, such as the use of delayed fluorescent materials [78–80].

3 Architecture

PLEDs are built so that thin-film layers overlap. Thus, an unlimited number of possible architectures can be varied: the number of layers, the thickness of the layers, and the material employed in each one. The devices may be assembled with one or multiple layers. In the simplest structure (monolayer), there is the electroluminescent layer between two injection electrodes (cathode for electrons; anode for holes).

This configuration usually has low quantum emission efficiency due to the disparity between electron and hole transport mobility, commonly observed in organic materials, which results in recombination distributed over the entire material length, which contributes to increased losses, as shown in Fig. 6.

In order to achieve high performance, one of the most effective strategies is to use multilayer structures, which can facilitate the injection of charges and confine the emissive layer (EML) excitons. While it is easy to make these devices, accurately controlling the thickness of the films is a challenge once the materials that make up the device layers, as they are solubilized to form the film, can cluster over the interface, thus preventing greater efficiency due to recombination of holes and electrons [81, 82].

In this sense, the devices can be constructed following a conventional or inverted configuration that differs by choice of the layer constituents and is discussed in the later items.

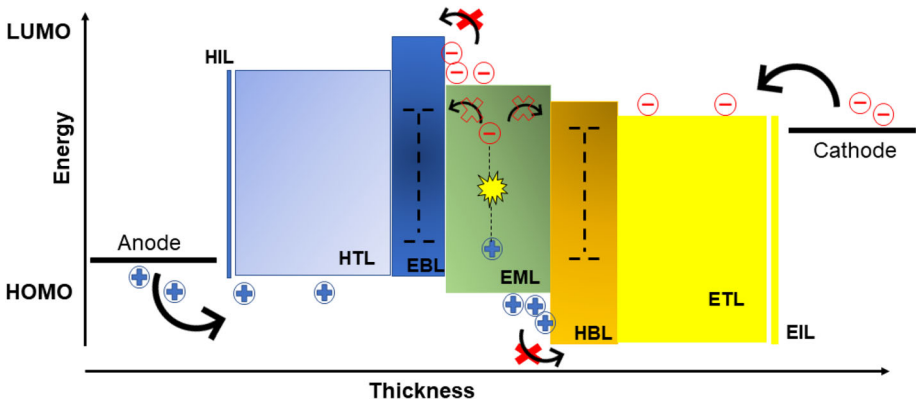

Fig. 5 Scheme of the electroluminescence process in an OLED device

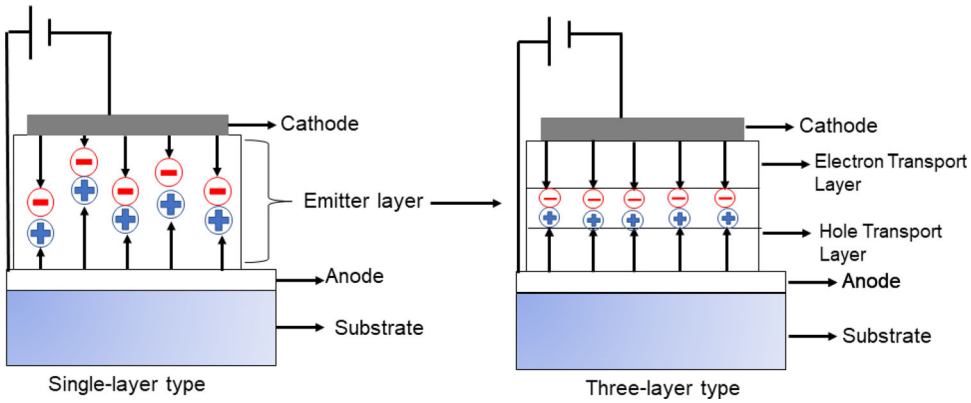

Fig. 6 Representation of charge recombination region in electroluminescent devices

3.1 Conventional configuration

In conventionally structured devices, there is usually substrate, anode, hole carrier layer (HTL), active layer (EML), electron carrier layer (ETL), and cathode. However, this type of architecture has some limitations associated with device degradation by air exposure, presenting long-term reliability problems. Such a configuration has low air stability and the device's operational life and, therefore, requires encapsulation to avoid degradation under oxygen and moisture [83, 84].

Another disadvantage presented for conventional PLEDs is how the emitted light must first travel through the ITO electrode and the glass to leave the device; thus, part of the light is retained in these layers. It limits the maximum external quantum efficiency (EQE that the device can have, in addition to the ITO's fragility, making it problematic to apply it to devices that require mechanical flexibility [85, 86].

Besides, the material employed as HTL is usually composed of PEDOT:PSS. Nevertheless, its conductivity is insufficient for many applications [87]. An example of the mentioned configuration can be observed in the work of Germino et al. [56]. They produced a PLED device based on a PVK composite and a salicylidene coordination compound, shown in Fig. 7. Their configuration consisted of an anode composed of ITO, the hole carrier layer of PEDOT:PSS, and the active layer by the PVK:salicylidene composite, which functions as a guest/host compound. Later, this device received calcium as an electron carrier layer, and as cathode, aluminum.

For this type of configuration, incorporating a host gives rise to a higher active layer emission.

3.2 Inverted configuration

To overcome the problems encountered in the conventional configuration, the inverted structure emerged, known as IBOLED (inverted bottom emitting OLED), which consists of a substrate, cathode composed of a TCO; electron injector layer (HIL), where a thin film of zinc or titanium oxide is usually employed; followed by the active layer responsible for the emission; the hole conveyor layer, made up of a thin film of vanadium or molybdenum oxides, which has good advantages such as mechanical and electrical durability, and transparency in the visible region. Finally, there is the anode, formed by a thin layer of aluminum. Such a configuration results in relatively high efficiency and stable emission spectrum [88, 89].

Inverted configuration devices have a lower cathode and an upper anode and have some advantages over conventional ones since inverted devices offer compatibility with n-type active matrix display technologies. In addition, the anode and cathode typically consist of thin layers of metal, which allow them to be used in flexible applications [90].

Examples of light-emitting devices with inverted configuration are presented in the works by Luo et al. [91]. They developed a PLED (Fig. 8) consisting of ITO as a cathode, followed by an electron injector layer based on a mixture of a dyed polybenzimidazole-based organic dye and zinc oxide (ZnO:PBI-H), an active layer of P-PPV, a hole carrier layer of molybdenum trioxide, and the aluminum anode.

This setting's choice is that the inversion of configuration causes an improvement of the electron injection in the device as the injection barrier is reduced. Therefore, there is a load balance in the

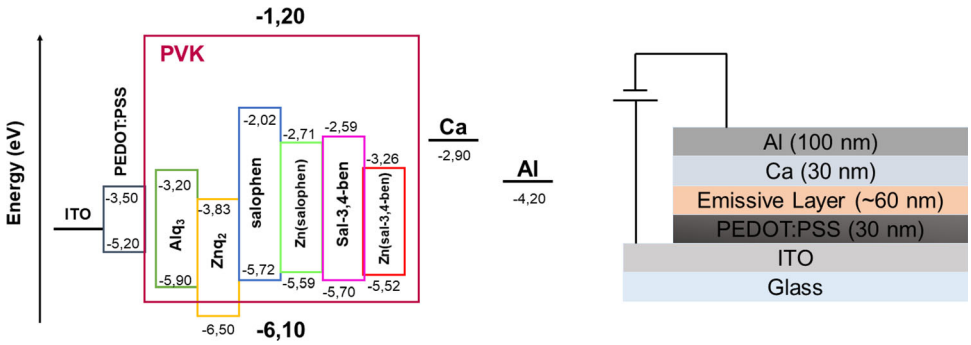

Fig. 7 Architecture of a conventional PVK:salicylidene device

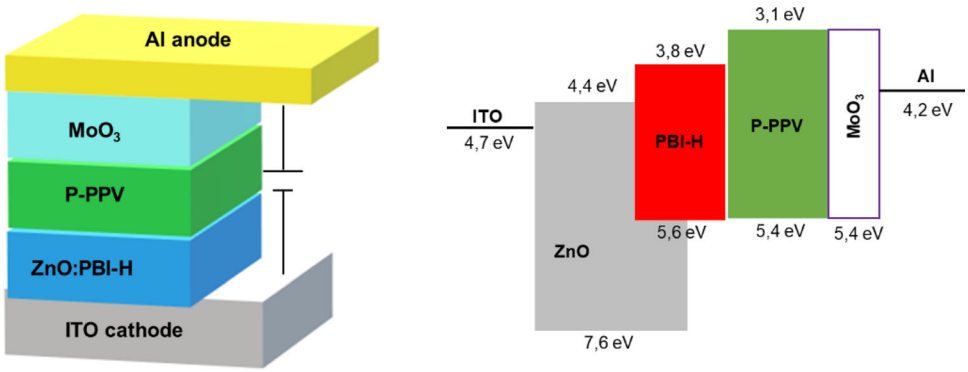

Fig. 8 Device configuration and the corresponding inverted PLED device power level diagram

emitting material, thus observing improvements in electroluminescence efficiency and brightness.

4 Organic light-emitting diodes (OLEDs) with thermally activated delayed fluorescence emitters (TADF)

These electroluminescence systems have gained prominence in research in the application in lighting and display [78, 92] since a TADF emitter can achieve 100% internal quantum efficiency without using noble metals such as iridium and platinum, converting triplet exocytes into a singlet [93], through reverse intersystemic crossing (RISC), which consists of a process in which a low energy state of the triplet exciton is thermally elevated to the singlet level, and the rotation configuration that used to be of triplet rotation is changed through the interaction of orbit rotation to the singlet configuration (Fig. 9). Thus, the fluorescence of these singlet states is moderately delayed, therefore receiving the name of thermally activated delayed fluorescence (TADF) [80, 94, 95].

The internal quantum efficiency consists of the ratio of photons generated and the number of carriers (electrons and holes). Efficiency data depends on the relative probabilities of the recombination processes, whether they are radioactive or not. They are subject to the device's structure, the type of impurities, and mainly the semiconductor material that comprises it [96, 97].

As seen in Fig. 9, the thermally activated mechanism corresponds to an intramolecular mechanism that generates delayed fluorescence. The TADFs are based on the occupation of vibrational and electronic triplet levels of greater energy through thermal activation accompanied by the intersystem crossing process (ISC) in order to convert excited triplet singlet states into excited singlet states that later recombine radiatively. This mechanism is inversely proportional to the energy gap between the triplet state (T1) and the singlet state (S1). Such an energy gap is known as Δ_{EST}. Thus, materials with a relatively small gap provide a greater conversion of the triplet-singlet type through TADF.

The TADF process is also related to the temperature of the sample, since the higher the temperature, the greater the occupation of the higher energy triplet states, and therefore, the greater the likelihood of

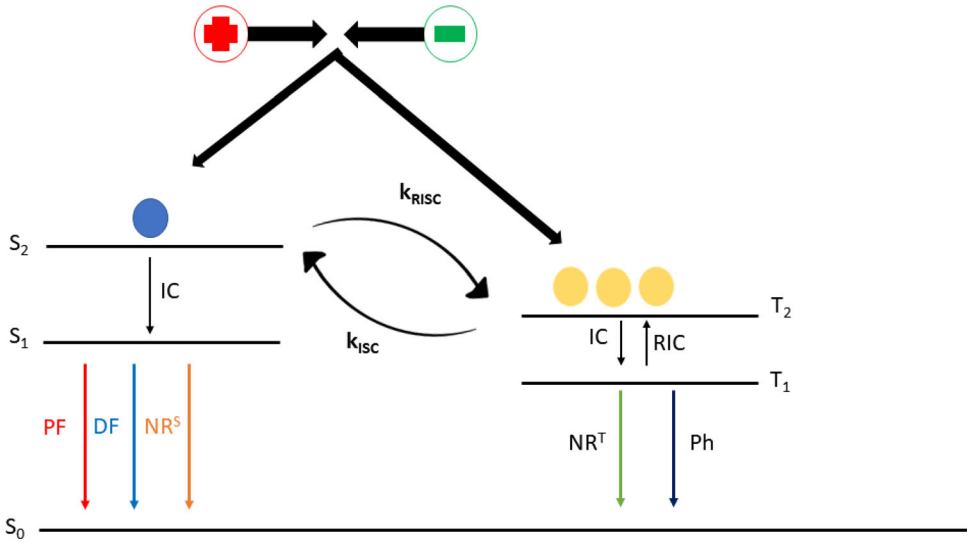

Fig. 9 Thermally activated delayed fluorescence mechanism (S_1 and T_1 lowest exciton states, *IC* internal conversion, *RISC* reverse intersystem crossing, *PF* prompt fluorescence, *DF* delayed fluorescence, *NR* decay or non-radioactive, *Ph* phosphorescence, *ISC* intersystem crossing, K_{ISC} rate constant of ISC, K_{RISC} rate constant of endothermic RISC, NR^S singlet nonradiative decay, NR^T triplet nonradiative decay, *RIC* reverse internal conversion

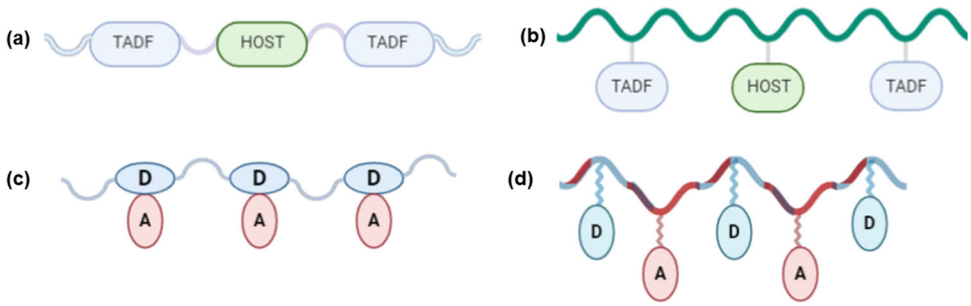

Fig. 10 Schematic representation of structural designs for solution-processable TADF polymers

reconversion between the excited singlet type states through reverse intersystem crossing (RISC) [92, 98].

In polymers, it can be carried out employing four strategies (Fig. 10), (1) TADF units (monomers) separated by flexible alkyl chains in an unconjugated polymer backbone [79], (2) TADF units can be grafted laterally to the polymer main chain (TADF unit as a pendant) [99, 100], (3) donor and acceptor units are alternately connected to the polymer backbone [101], and (4) donor units are attached to the polymer main chain, while acceptor units are grafted adjacent to the donor units in the polymer chain [102–106].

Thus, there is a growing interest in developing such materials and adapting them for processing in a solution that has been widely used in large-area devices [107, 108].

Examples of the proposed structures of TADF polymers are reported in the work of Yang et al. [109], when they develop a series of conjugated polymers based on the backbone-donor/pendant-acceptor (BDPA) strategy, where benzophenone was used as an accepting group in polymers that had the carbazole/acridine donor as the backbone in which unit 9,9-dihexyl-10-(4′-benzophenone)-9,10-dihydroacridine (ABP) (Fig. 11) was added to the conjugated skeleton using its donor fraction, generating the PABPC copolymers.

Using such a strategy, the authors achieved Δ_{EST} small, high quantum photoluminescence yields (PLQYs) of up to 0.77 in pure film, and when used in light-emitting devices, a high EQE of up to 18.1% was reported (Fig. 12).

This achievement was reported for the copolymer PABPC5, which corresponds to the sample with 5% molar content of the ABP unit, indicating that the proportion of the delayed component of the TADF

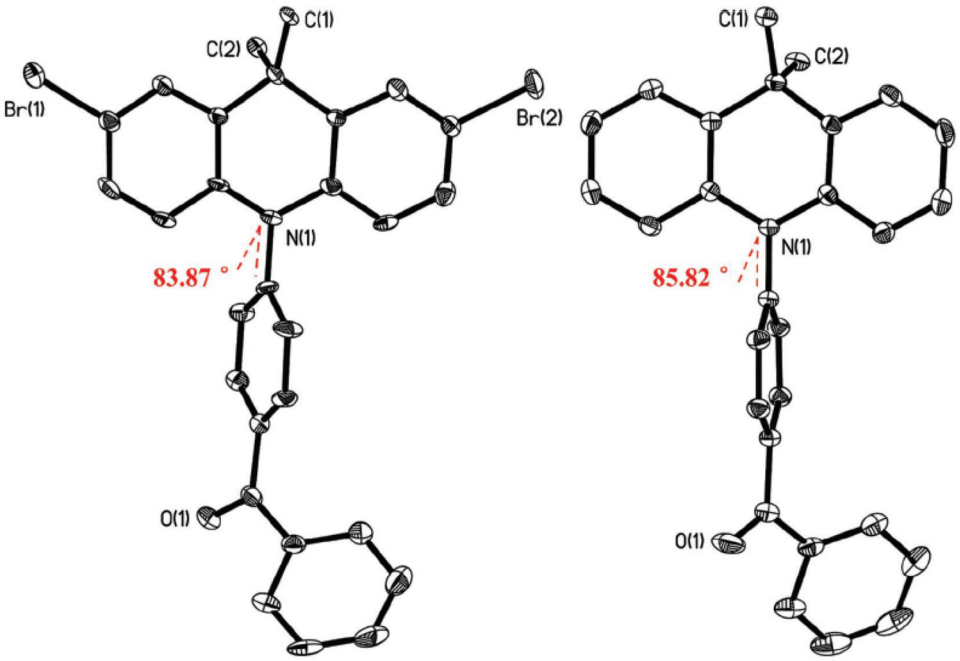

Fig. 11 Crystalline structure of the 9,10-dihydroacridine derivative (M1) monomer and ABP precursor with strong torsion between the acridine and benzophenone groups [109]

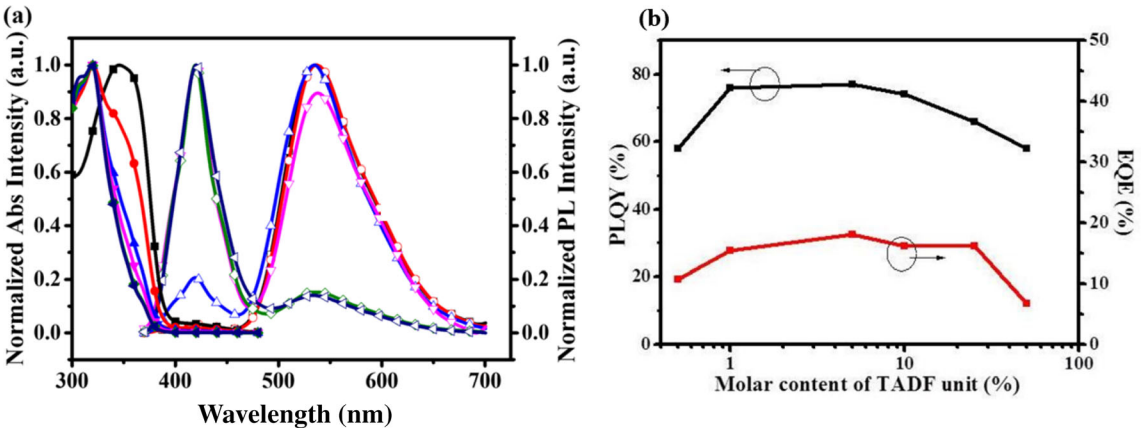

Fig. 12 **a** Absorption (square: PABPC50; circle: PABPC25; trianlge: PABPC10; inverted triangle: PABP5; diamond: PABPC1 and left pointing arrow: PABPC0.5) and PL spectra of polymers with ABP units performed in atmosphere and atmosphere at 300 K (open symbols). **b** Photoluminescent quantum yield (PLQY) and external quantum economy (EQE) for TADF polymer emitters as a function of the unit's molar content ABP (adapted from information support [109])

emitter increases as the concentration of the ABP unit in the molecule is lower. In addition, it was observed that the increase in temperature from 50 to 300 K increases the delay, which was expected for TADF emitters since the conversion of the triplet states (T1) into singlets (S1) is thermally activated.

In turn, Wei et al. [104] proposed a new methodology for the synthesis of a TADF polymer with units that alone do not have such behavior (Fig. 13), the polymer was designed by combining benzophenone units (electron acceptors) and carbazole units (electron donors) twisted together.

With the methodology developed, the authors reported that the polymer produced showed solvatochromic behavior under irradiation, with fluorescence emission in the blue to yellow range according to the solvent, which can be, toluene, THF, orthodichlorobenzene (ODCB), chloroform, and dichloromethane (DCM), indicating potential TADF occurrence, since, a singlet excitation of the lower load transfer type occurs. As seen in Fig. 14, P1

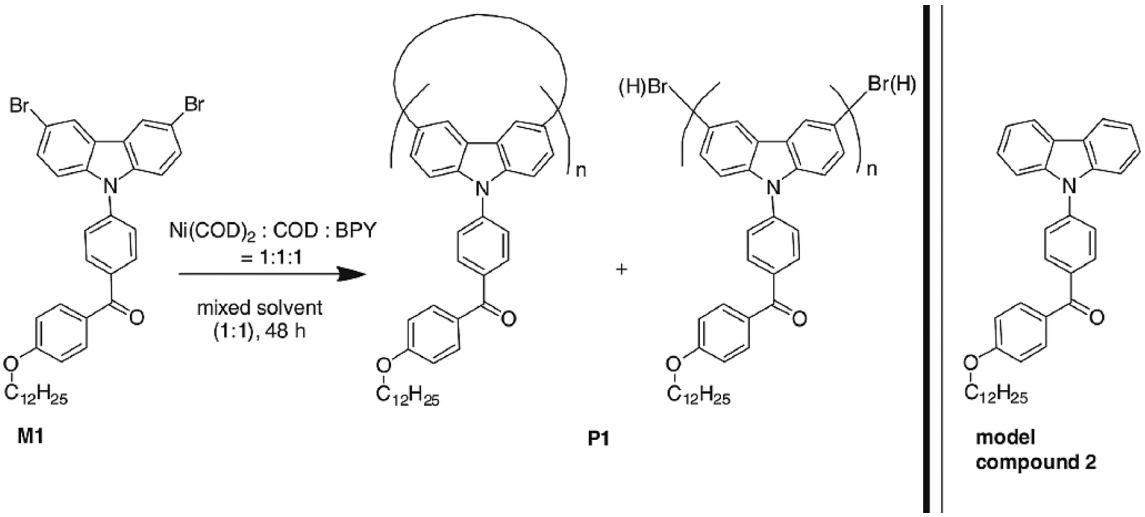

Fig. 13 Synthesis of the P1 polymer using the monomer [4-(3,6-dibromo-carbazol-9-yl)phenyl][4- (dodecyloxy)phenyl]methanone (M1) and possible structures [104]

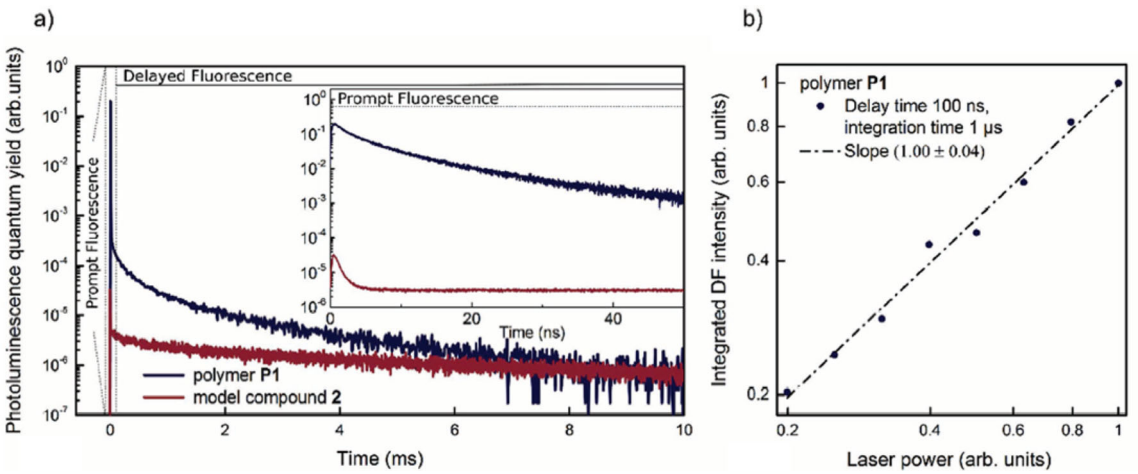

Fig. 14 **a** Time-resolved photoluminescence for P1, as well as quantum photoluminescence yields measured under illumination **b** dependence on delayed fluorescence integrated by excitation power [104]

presents a delayed component of a biexponential character with an average life-weighted intensity of $\tau DF = 296 \pm 16$ µs, with the respective lifetimes of the fast and slow components being τDF, $1 = 52 \pm 8$ µs and τDF, $2 = 353 \pm 19$ µs, while in Fig. 14b, a linear proportionality between delayed fluorescence and excitation power is demonstrated, indicating an upward conversion process a single photon, consistent with the TADF process [104].

In this way, it is possible to demonstrate that it is possible to achieve polymers with TADF properties based on units that do not have such a characteristic, which favors the chemical and technological development of new materials.

Another strategy developed to reach TADF polymers is the side chain's engineering since the main polymer chain can inherit the laterally grafted TADF units' characteristics. In this sense, Zhou et al. [110] developed a series of polymers that constituted the main backbone of a copolymer comprising in fractions of unconjugated tetraphenyl silane and conjugated carbazole unit.. In contrast, the side chain was composed of *10,10′-(2-(4-(9H-carbazol-9-yl)phenyl)pyrimidine-4,6-diyl)bis(4,1-phenylene))bis(10H-phenoxazine)* (PXZ-Pm-MeOCz), a classic TADF unit. The polymers were

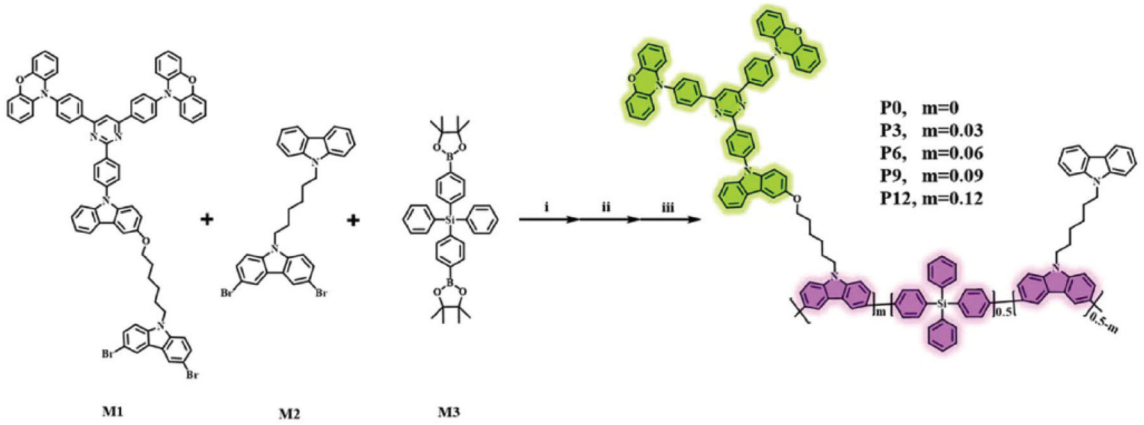

Fig. 15 Synthetic route for the TADF polymers based on carbazol and tetraphenyl silane (M1:10,10′-((2-(4-(3-(((6-(3,6-dibromo-9H-carbazol-9-yl)hexyl)oxy)-9H-carbazol-9-yl)phenyl) pyrimidine-4,6-diyl)bis(4,1-phenylene))bis(10H-phenoxazine) M2: 3-methoxy-9H-carbazole, 2-chloro-4,6-bis(4-chlorophenyl)pyrimidine, 3,6-dibromo-9-(6-bromohexyl)-9H-carbazole, 9-(6-(9Hcarbazol-9-yl)hexyl)-3,6-dibromo-9H-carbazole M3: diphenylbis(4-(4,4,5,5-tetramethyl-1,3,2-dioxaborolan-2-yl)phenyl)silane) (adapted from [110])

synthesized by Suzuki polycondensation of monomers M1, M2, and M3 with molar ratios of 3:47:50 (P3), 6:44:50 (P6), 9:41:50 (P9), and 12:38:50 (P12) (Fig. 15), and the polymer chain without the M1 TADF unit, that is, P0, was synthesized for comparison.

The polymers produced by the authors [110] were evaluated for transient photoluminescence decays from 100 to 300 K to verify TADF properties. Thus, the polymers revealed typical second-order exponential decays (Fig. 16) with fluorescence life of 24 to 25 ns and fluorescence life delayed from 1.9 to 2.6 μs at room temperature.

As the temperature was increased, the delayed fluorescence intensities were higher, indicating that the RISC channel from the triplet state (T1) to the singlet state (S1) can be thermally activated. Thus, the TADF characteristics were present in the polymers produced.

Zhou et al. [108] introduced the Friedel–Crafts polyhydroxyalkylation of carbazole and isatin to make TADF polymers interrupted by conjugation. Thus, TADF units composed of *9,9-dimethyl-9,10-dihydroacridine* (DMAC) to *diphenyl sulfone* (DPS) and *carbazole* (DMAC-DPS-Cz) were introduced into the polymer skeleton, forming the PACDPS polymer with molar proportions of the monomers M1:M2:M3 of 5:95:100 (PACDPS-5), 10:90:100 (PACDPS-10) and 15:85:100 (PACDPS-15) (Fig. 17).

The TADF properties of the polymers produced were evaluated according to measurements of photoluminescence transients in doped films, which revealed second-order exponential decays with fluorescence times of 16 to 17 ns and delayed fluorescence lifetime of 1.2 to 1.3 μs (Fig. 18).

Such a methodology for producing TADF polymers proved that TADF polymers are effective. It produces polymers with delayed fluorescence properties with a synthetic route and simple purification compared to the commonly used coupling reactions.

Therefore, the development of TADF polymers and the most diverse structures to achieve such a property opens a field of innovations, given that, by synthesizing the acceptor and donor units or even the polymeric skeleton, they can modify an entire system and thus, there are differentiated photoluminescence, quantum efficiency, and electroluminescence responses, in order to be a possible substitute for the phosphorescent materials so commonly used [79, 111–113].

Wang et al. [114] developed a copolymer consisting of alternating units of fluorene and dibenzothiophene-S, S-dioxide (SO) together with the 2-(4-(diphenylamino)-phenyl)-9H-thioxanthen-9-one-10,10-TADF unit dioxide (TT), generating the polymer TADF PFSOTTx (Fig. 19) to achieve the emission of white light, solely by this polymer.

Through thermal analysis, it was possible to evaluate that the conjugated polymers produced (PFSOTT0.05-PPSOTT10) have good thermal stability, with a decomposition temperature of about 410 °C. The devices produced having the copolymers had the following composition, ITO (anode)/PEDOT:PSS

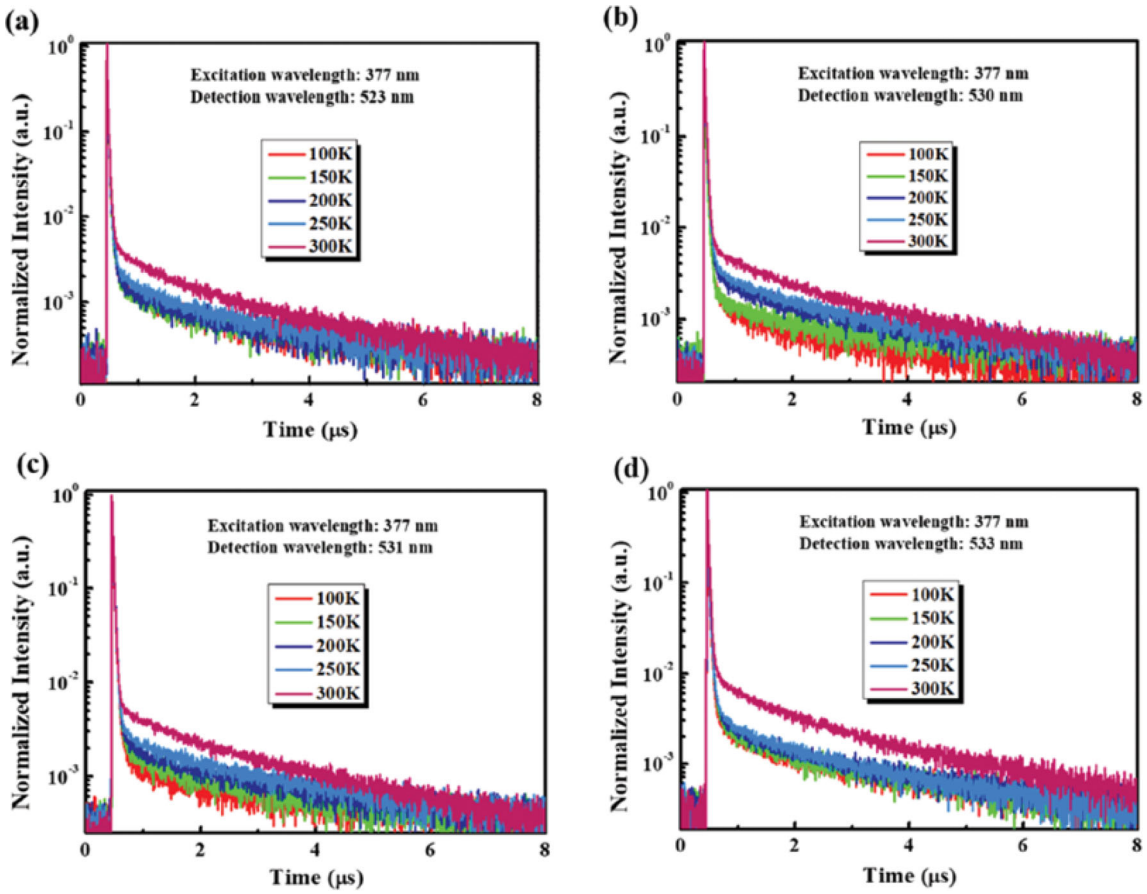

Fig. 16 Transient decay spectra of PL as a function of temperature (100 to 300 K) of polymers **a** P3, **b** P6, **c** P9, and **d** P12 [110]

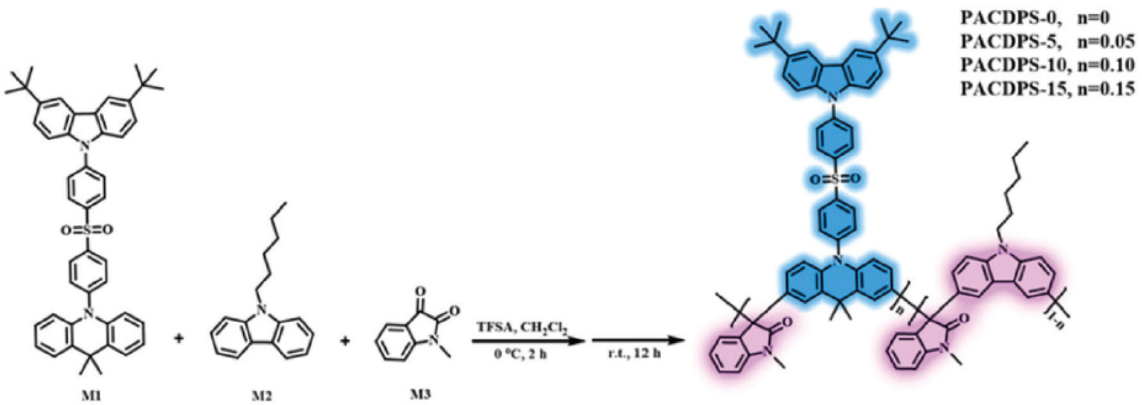

Fig. 17 Synthesis of TADF polymers based on 1-bromo-4-((4-fluorophenyl)sulfonyl)benzene (M1), 9-hexyl-9H-carbazole (M2) and 1-methylindoline-2,3-dione (M3)

(injection of holes)/TFB (layer hole carrier)/EML (PFSOTT)/TmPyPB (electron carrier layer)/Liq (electron injector layer) and Al (cathode).With a concentration of 2% of the TADF component (PFSOTT2), it was possible to reach a device that presented warm white electroluminescence and about 10% EQE (Fig. 20).

The EL spectra of PFSOTT0.05 and PFSOTT0.1 (Fig. 20c) exhibit simultaneous blue emission at 438/440 nm of the backbone and orange emission at 590/592 nm from the TADF unit, which corresponds

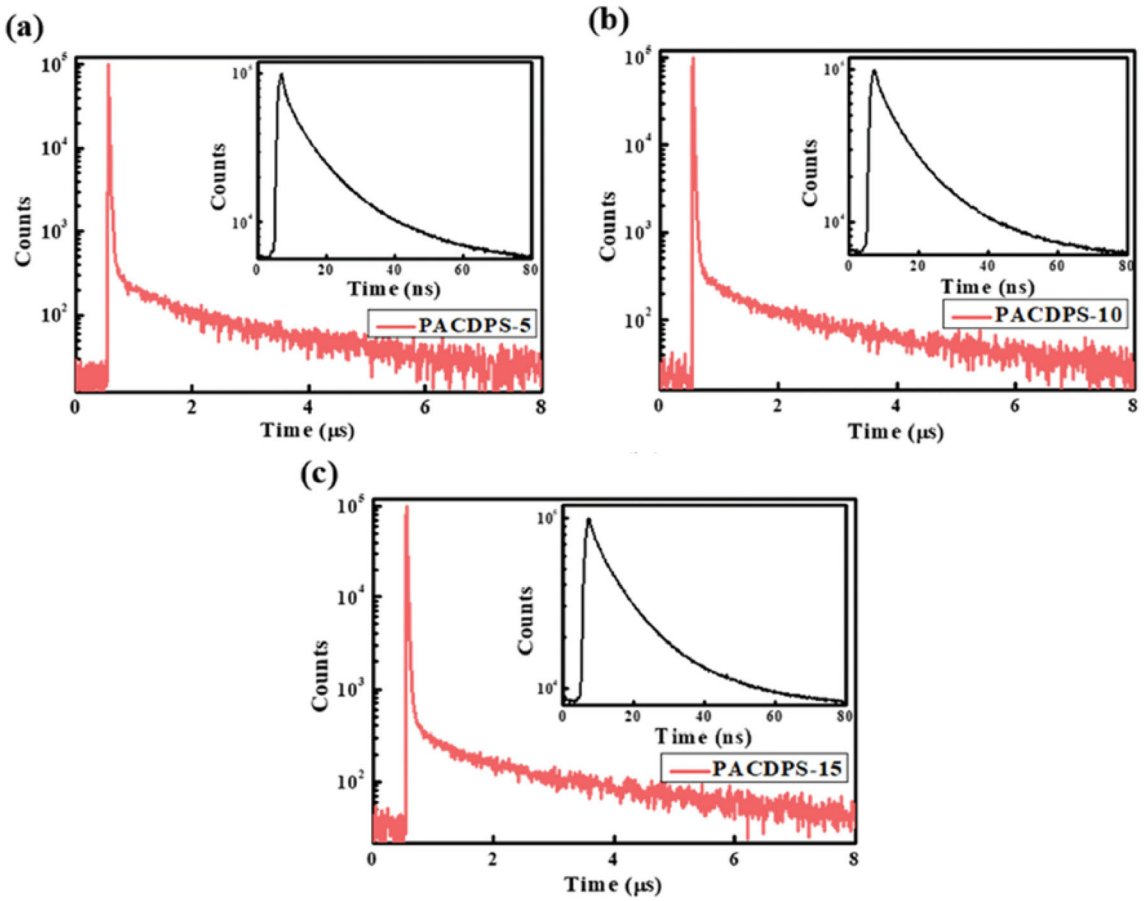

Fig. 18 The PL transient decay spectra of **a** PACDPS-5, **b** PACDPS-10 and **c** PACDPS-15 [108]

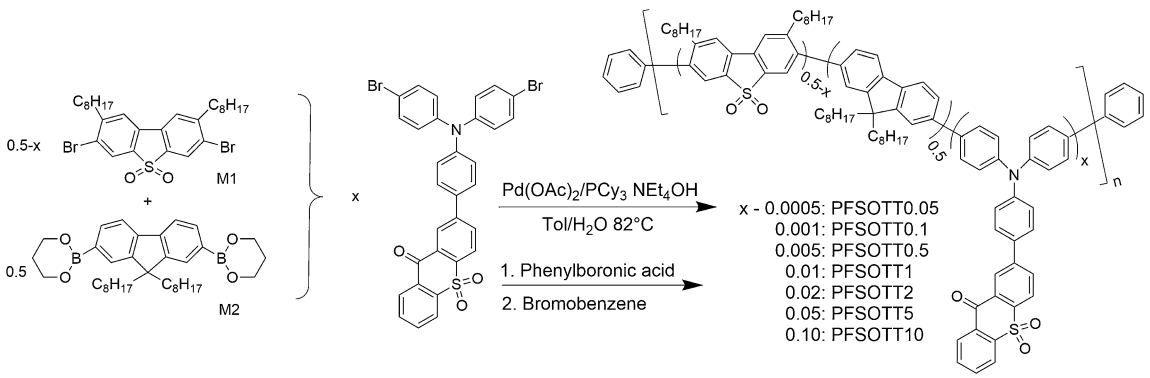

Fig. 19 Suzuki coupling reaction of PFSOTTx copolymer (adapted from [114])

to the coordinates of the Commission Internationale de L'Eclairage (CIE) (0.32, 0.31) and (0.36, 0.36), respectively, which are close to the emission of pure white light (0.33, 0.33). By optimizing the device's structure using 1,3-bis(N-carbazolyl) benzene (mCP) as a dopant mCP in the emitting layer, the EQE max increased to 19.4%.

Li et al. [112], in turn, synthesized white doped OLEDs based on terminally activated fluorescence polymers consisting of a polyethylene backbone and pendants of 2-(9,9-dimethyl-acrin-10-yl)-8-vinyldimethyl thioxanthene)-S,S-dioxide (DMA-TXO$_2$), 9,9-dimethyl-10-(3-vinylphenyl)-9,10-dihydroacridine (BDMAc) and 2-(10H-phenothiazin-10-yl)-8-vinyldibenzothiophene-S,S-dioxide, generating the PDTPT emitting layer (Fig. 21).

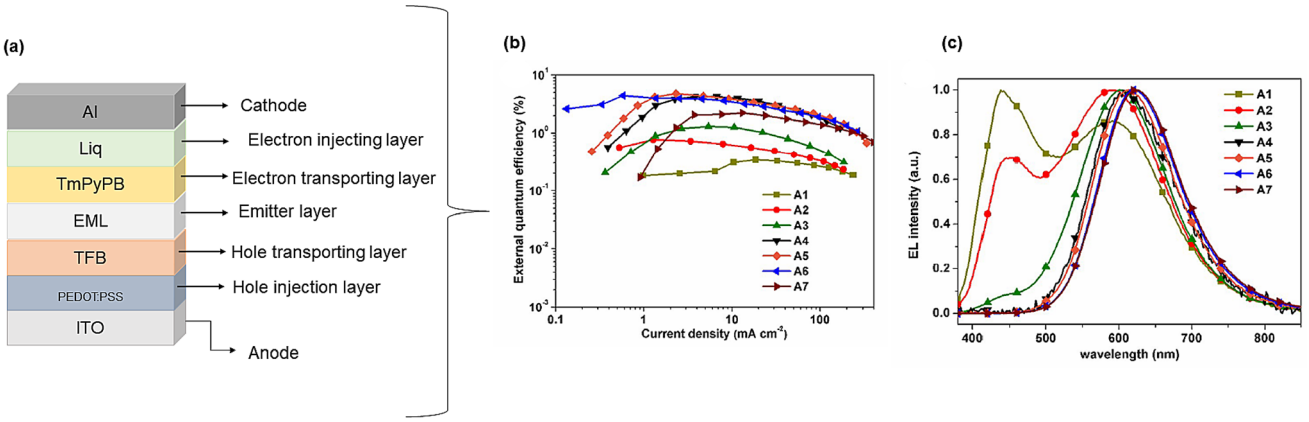

Fig. 20 **a** Device structure, **b** external quantum efficiency and **c** current density plots for the devices (adapted from [114])

The project developed by the authors is based on the use of host units (BDMAc and DMATXO2) emitting deep blue light and accepting (PTZ-DBTO2) emitting yellow light in order to achieve white light with the combination of blue and white chromophores yellow-orange.

Figure 22 shows the electroluminescence and external quantum efficiency spectra. The device produced (PDTPT-1) reaches a maximum luminance of 2900 cd m^{-2}, a maximum current efficiency (EC) of 38.8 cd A^{-1}, a maximum energy efficiency (PE) of 20.3 lm W^{-1} with CIE coordinates of (0.33, 0.42). The PLED device composed of the PDTPT-1 emission layer showed an external quantum efficiency of 14.2%, max photoluminescence of 20.3 lm W^{-1}, and CIE coordinates (0.33, 0.42) and (0.31, 0.39). Thus, demonstrating that the strategy developed in the emission layer's construction promises to obtain white WOLEDs of high efficiency and low production cost.

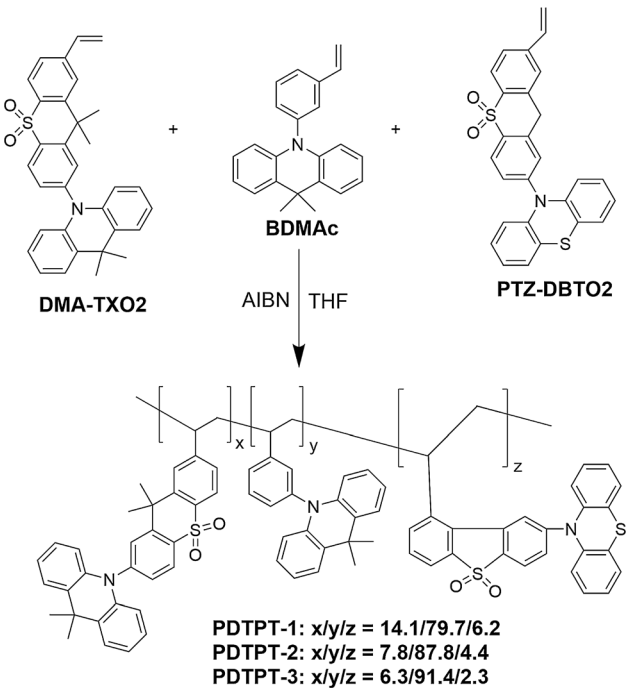

Fig. 21 PDTPT polymer synthetic route

As the synthesis of compounds based on white emission TADF is still a challenge since the molecules can aggregate through the π-π interactions causing excitonic losses [115–117]. From this perspective, Kubo et al. [118] report structures that show delayed fluorescence by aggregation-induced emission (AIE-DF). To achieve a structure containing such groups, the concepts of supramolecular polymerization [119–121] were used. It is possible to adjust the proportions of chromophores in the polymer and their properties through chemical stimuli. The interactions between the groups are non-covalent and highly directional and reversible.

An example of a supramolecular structure is reported by Schubert et al. [122]. They developed Zn^{2+} bisterpiridine based polymers in which the dynamic nature of the Zn^{2+} complex allowed the systematic assembly of statistical copolymers. Such an approach led to the production of specific emission colors for the intended application. The structure developed is shown in Fig. 23.

The elaborated structure (metallopolymers) allowed the assembly of different chromophores in different proportions, and these are capable of emitting simultaneously at different wavelengths and consequently producing the white moon. This adopted strategy is efficient because it does not use

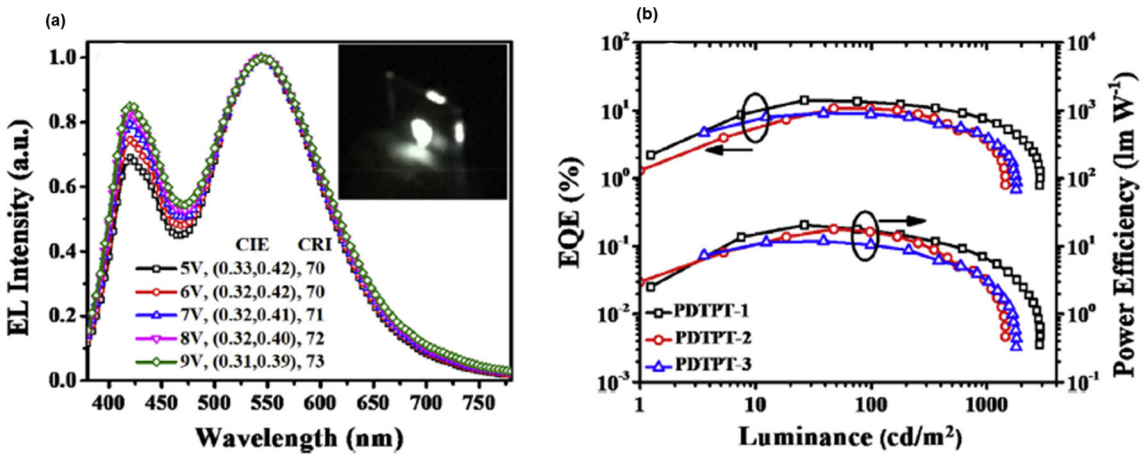

Fig. 22 **a** EL spectra of PDTPT-1 at different voltages, **b** EQE and energy efficiency *vs.* luminance for PDTPT-1 (adapted from [112])

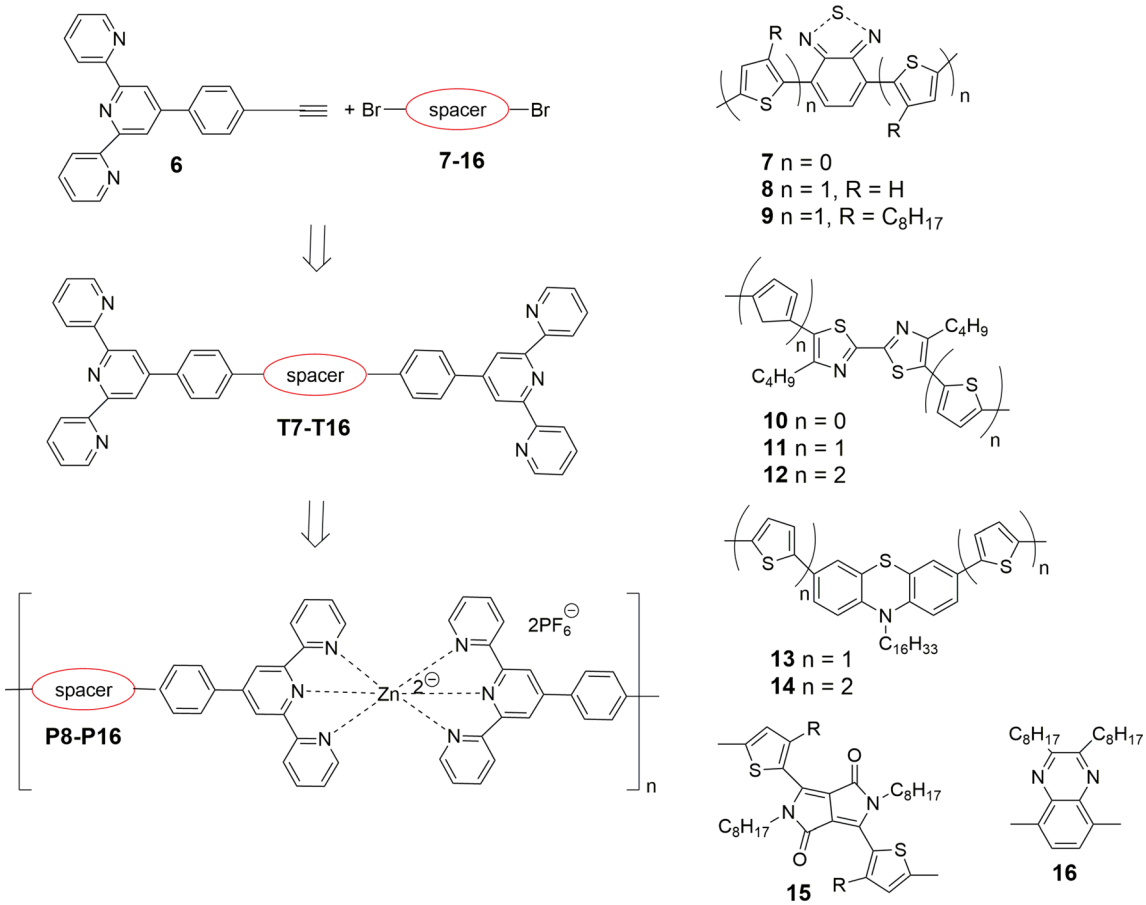

Fig. 23 Schematic representation of the synthesis of bisterpiridines (T7 to T16) and the coordinating polymers of Zn^{2+} (P8 to P16)

expensive heavy metals, as well as adapting the emission in a single polymeric system.

5 Solid-state lighting

Solid-state lighting (SSL) is an alternative, environmentally friendly lighting technology that has become more noticeable as concerns about conventional power sources' environmental impact have

increased. Thus, numerous researches have been conducted to develop intelligent ways to use electric power [51, 123, 124]. In SSL, the illumination is obtained through semiconductor devices, such as inorganic light-emitting diodes (LEDs), organic ones (OLEDs), as well as polymeric ones (PLEDs), the latter being of interest to the present research review. Such devices provide visible light through the electroluminescence process, and their main advantage over incandescent and fluorescent lamps is their higher energy conversion efficiency and service life.

PLEDs are optoelectronic devices formed by thin films of emitting polymers that make up the active layer. As an electric current is supplied, the charge carriers walk through the device structure and recombine in the emitting layer. The emitted color and the intensity of the colors and brightness is dependent on the electric current supplied. They are versatile, self-emitting, temperature resistant, and require thinner layers than conventional lighting technologies [125–127].

For application in solid-state lighting, devices must meet certain requirements, and these are: display color quality, including appropriate color temperature (CT), and have high color rendering index (CRI) [43]. The desired emission is white light, as it most closely resembles natural light.

6 White light

White light can be obtained from various device configurations. These devices should generate light with a similar spectral distribution to natural light, covering most of the visible spectrum [128, 129]. White light-emitting devices having a polymer emitting layer are called WPLED [130, 131].

The configurations adopted by these devices for the formation of white light may comprise the mixing of two or more polymer systems or a single polymer where their chromophores emit in the red, green, and blue (RGB) emission range [132, 133]. Three factors characterize white these being the (1) coordinates of the Commission Internationale de l'Eclairage (CIE) of (0.33, 0.33), (2) the correlated color temperature (CCT), and (3) the color rendering index (CRI), which determines how the color of an object appears under illumination, that is, a source of a black body (CRI = 100) [134, 135].

For lighting applications, the light-emitting device should reveal coordinates closer to the ideal white point, with CRI above 80 and CCT similar to blackbody radiation between 2500 and 6500 K. These requirements are important for the best color purity [136].

To achieve such conditions, several designs have been proposed, among them are those presented in Fig. 24, where there are (A) single-layer devices, which consist of an active layer composed of a mixture of materials that exhibit several bands of issuance; (B) multilayer systems, where each layer is composed of electroluminescent polymers; (C) the arrangement of the tandem layers; (D) structure manufactured laterally; and (E) a monolayer consisting of a polymer that emits in a wide range of the visible spectrum [25, 133, 137–139].

The approaches white light generation utilizing RGB emitters tend to provide it in a purer form. However, they still have low electroluminescence efficiency and, therefore, there is still much to be done in this direction [140]. The most recent advances in RGB devices in terms of performance and structure are described in the following item.

7 RGB device designs

The device structures that employ RGB emitting layers can assume five different designs. An example of the design reported in Fig. 25e can be understood in the work of Liu et al. [141] when they developed a unique polymer system in the form of a star with simultaneous RGB emission (Fig. 25). The red-emitting core is composed of a dopant formed by tris (4-(3-hexyl-5-(7-(4-hexylthiophen-2-yl)-benzo[c][1,2,5]thiadiazole-4-il) thiophen-2-yl) phenyl) amine (TN), by emitting arms in blue, composed of polyfluorene (PF) and green-emitting dopant of benzothiadiazole (BT).

A greater energy transfer can be guaranteed by carrying out such a strategy, resulting in higher white light emission. This transfer is controlled by the concentration of TN and BT. In this way, the device developed obtained high-quality white color, with CIE coordinate of (0.34, 0.35) and current efficiency of 2.41 cd A^{-1}.

Zou et al. [142] developed a device in which the active layer was formed by the mixture of electroluminescent polymers (Fig. 26), which contained

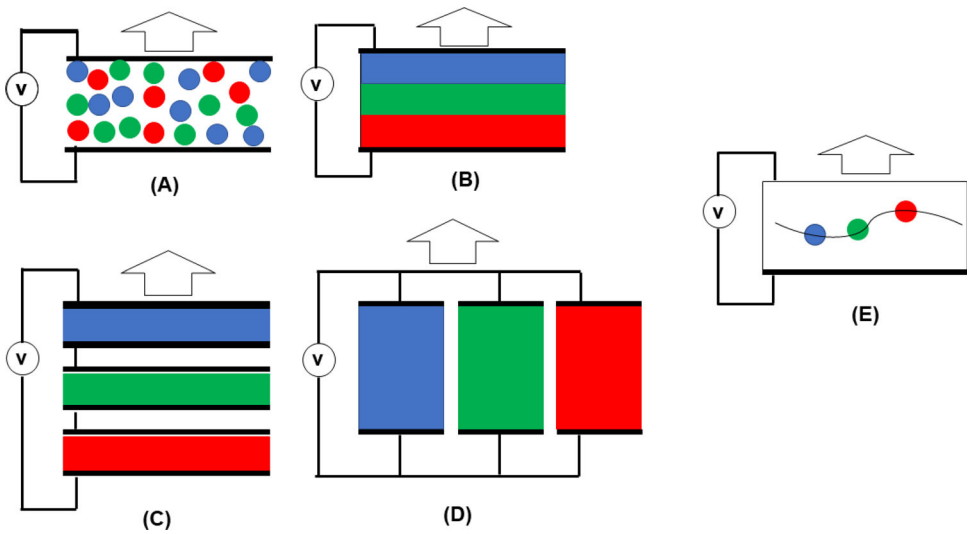

Fig. 24 Representation of devices used to generate white light from PLEDs: **a** single EML structure, **b** multilayer EML structure, **c** stacking and tandem structure, and **d** side structure, **e** monolayer structure with the range of visible light

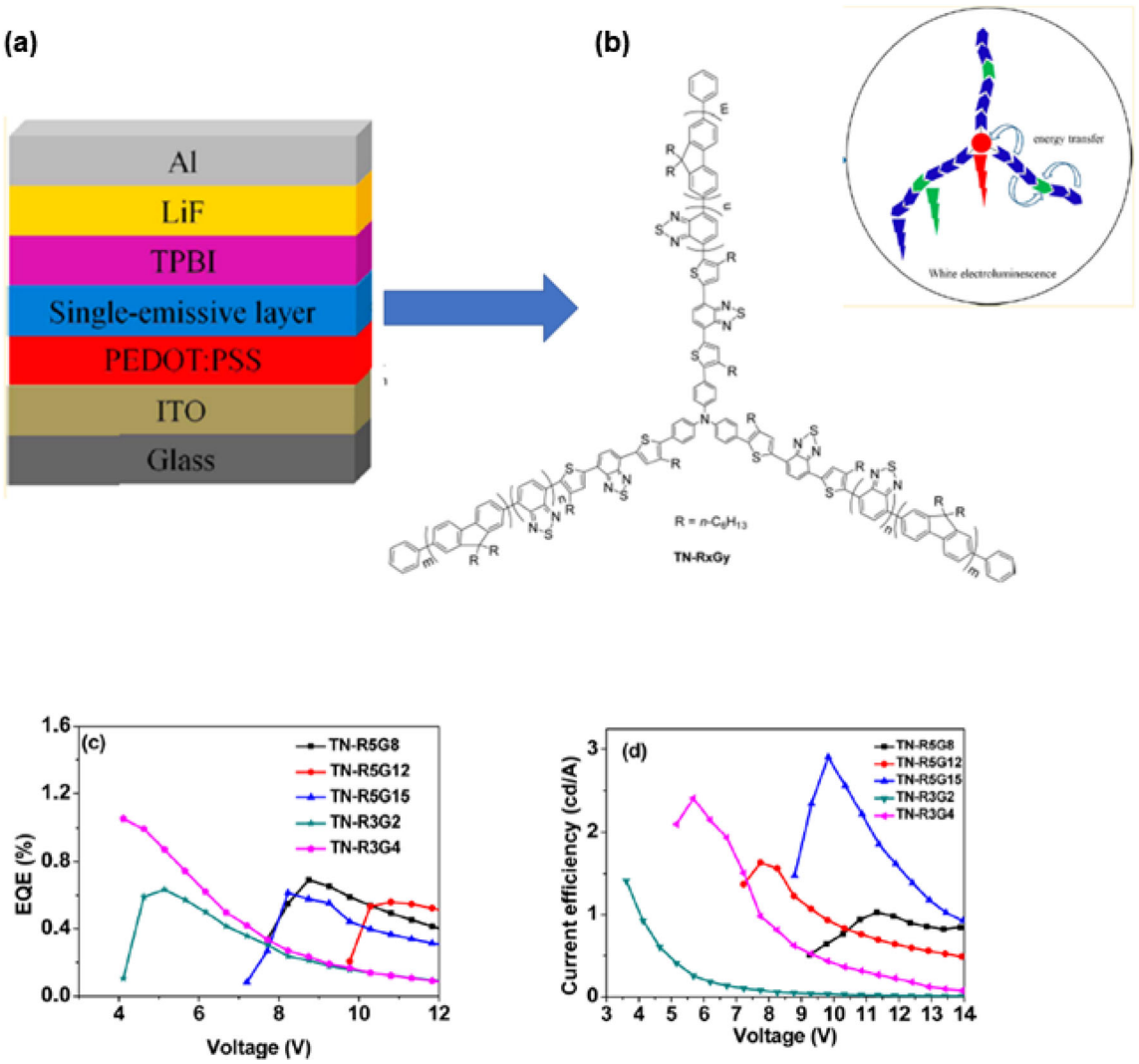

Fig. 25 Schematic illustrations of the device consisting of a star polymer—TN-RxGya (**a**) device (**b**) star-shaped single polymer **c** EQE − voltage characteristics; **d** current efficiency − voltage characteristics (adapted from [141])

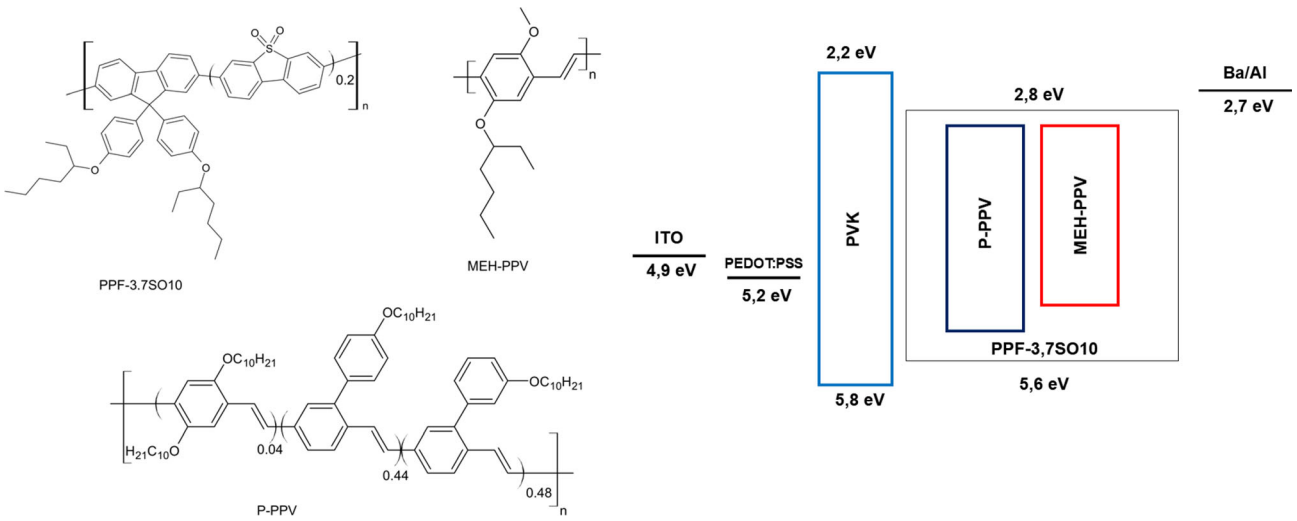

Fig. 26 The chemical structures of PPF-3,7SO10, P-PPV and MEH–PPV device and energy diagram of the device made with PPF-3.7 SO10:P-PPV:MEH-PPV

poly[2-methoxy-5-(2-ethylhexyloxy)-1,4-phenylenevinylene] (MEH-PPV), poly(p-phenylene vinylene) (PPV) and poly[(9,9-*bis*(4-(2-ethylhexyloxy) phenyl)fluorene)-co-(3,7-dibenziothiene-S,S-dioxide10)] (PPF-3,7SO10), emitting the colors red, green and blue, respectively.

With the developed device, balanced white electroluminescence spectra were obtained, with CIE coordinates (0.331, 0.353) very close to pure white, with a mixing ratio of 100:0.8:0.5 (by mass) between the polymers RGB, achieving high electroluminescence efficiencies of 14.0 cd A^{-1}, which corresponds to a quantum efficiency of 6.9% at a current density of 10 mA cm^2.

In addition, it has a CRI of 79 and a color temperature of 2800–6600 K; that is, such parameters have been shown to be suitable for applications in solid-state lighting.

Gather et al. [44] developed a device in which the RGB electroluminescent polymers were placed laterally on the layers (Fig. 27). This arrangement was achieved through the polymers crosslinking mixed with small amounts (< 0.5% by mass) of a photoacid, which donates a proton after exposure to UV light. Exposing only a few polymeric film areas through a shadow mask, the researchers could selectively crosslink. The crosslinking makes the films insoluble, and in this way, the polymers can be directly structured via photolithography.

The authors' devices' emission profile can be defined for any color within a wide range of colors and is maintained in several orders of magnitude in brightness by a simple but efficient adaptation system. With the developed design, characteristics of a white light emission device with CIE of (0.33, 0.33) and an efficiency of 5 cd A^{-1} were achieved.

Zhu et al. [143] developed a device consisting of a host material based on a spiro backbone and incorporated a tercarbazole donor to apply organic phosphorescent light-emitting diodes RGB type. Such a structure is proposed since it reduces the energy loss caused by an induced collision. In work developed, a new host 3,6-di(9H-carbazol-9-yl)spiro[indolo[3,2,1-

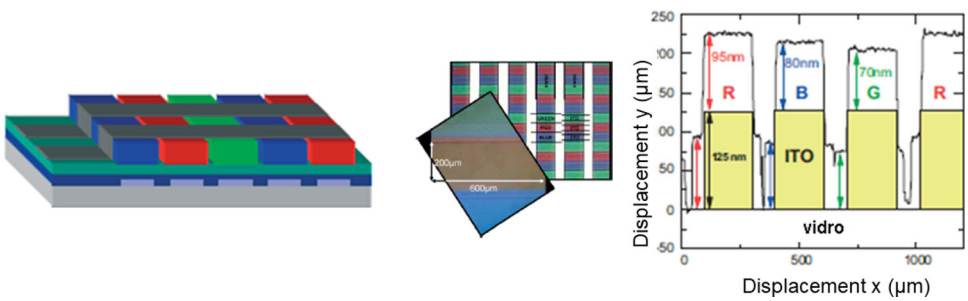

Fig. 27 Schematic representation of the structure of the reticulated RGB device with photolithography (adapted from [44])

de]acridine-8,9′-thioxanthene]10′,10′-dioxide (TCZSO2) was synthesized, and the 9′H-9,3′:6′,9″-tercarbazole acceptor was fused to the structure, demonstrating that the modifications made to the structure reveal promising properties, such as efficiencies of 22.8% and 24%, respectively, when applied as a host for devices based on Flrpic and $Ir(ppy)_2(acac)$.

The elaborated device is shown in Fig. 28, where it is possible to notice that the electrode was composed of tin-doped indium oxide (ITO), a 1,4,5,8,9,11-hexaazatriphenylene-hexacarbonitrile layer (HAT-CN) that had the function of injecting holes, over it, a layer of 1-bis((di-4-tolyl-amino) phenyl)cyclohexane (TAPC) and 4.4′,4″-tris (*N*-carbazolyl)triphenylamine (TCTA) and light-emitting materials, bis(4,6-(difluorophenyl)pyridinate-N,C2′)picolinate (FIrpic) blue emitter, Iridium(III)-bis(2-phenylpyridinato-N,C2′)acetylacetonate (Ir $(ppy)_2$acac, green emitter and red emitter based on Iridium(III)-bis(2-methyldibenzo [f, h] quinoxaline acetylacetonate, a hole blocking and electron transport layer have been added over the emitter layers, consisting of 1,3,5-tri [(3-pyridyl)-phenn-3-yl (TmPyPB) and finally the 8-hydroxyquinoline (Liq) layers, responsible for the electron injection and finally the cathode aluminum (Al).

The developed strategy revealed better performances than the devices reported in the literature so far. For the red light-emission device with TCZSO2 host, the EQE was 21%, while for green and blue emitters, efficiencies of 24 and 23% were achieved, respectively. It is also demonstrated that films developed with this host showed better homogeneity than films based on 1,3-di (9H-carbazol-9-yl) - benzene (mCP), associated with the high Tg of spiro-type materials where TCZSO2 was grafted.

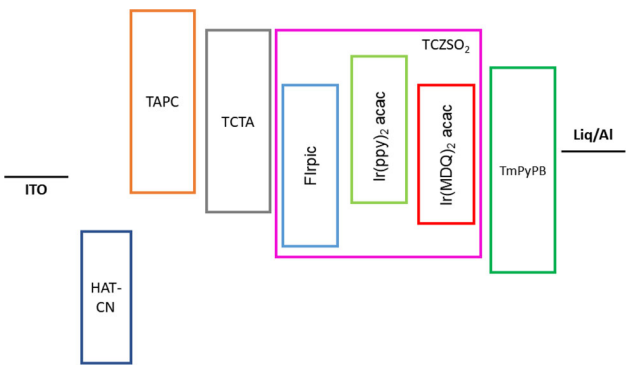

Fig. 28 PHOLED RGB device structure based on spiro host material and tercarbazole donor (adapted from [143])

Yin et al. [144] propose a WRGB emitting device employing a blue OLED used as a pumping source (BOLED) as a conversion layer based on quantum dots. The authors developed a device employing a PMMA micropillary matrix and red quantum dots of cadmium selenide (CdSe) and green zinc sulfide (ZnS) incorporated in the polymeric matrix. Therefore, descending conversion films were proposed using blue-emitting OLEDs integrated with a color filter (Fig. 29).

The pumping system consisted of a glass substrate, where a layer of tin-doped indium oxide (ITO) was deposited, and on top of it, a layer of molybdenum oxide (MoO_3), a layer of 1-bis[(di- 4-tolyl-amino) phenyl] cyclohexane (TAPC), a 4.4′,4″-tris(N-carbazolyl) triphenyl-amine (TCTA) layer, then a 1,3,5-tri[(3-pyridyl)-phen-3-yl]benzene (TmPyPB), therefore a layer of lithium fluoride (LiF), ending with an electrode layer composed of Mg:Ag in the proportion of 6% by mass.

The production of a device that consists of micropillars revealed improvements in efficiency in the extraction of light since part of the photons retained in the substrate and in the films are extracted into the air by means of the micropillars, thus ordering the matrices.

When employing RGB color filters with micropillary arrangements, each filter allows the passage of a specific wavelength. Thus, the RGB device with QDs is stable when subjected to different voltages, presenting a narrow color spectrum, whose range of colors reaches up to 83.1% National Television System Committee (NTSC), that is, with the data obtained, it would be possible to apply it to color monitors.

Zhao et al. [145], aiming to control the formation of excimers in host materials since they impact the efficiency of the emitting materials, and thus, it is an undesired phenomenon, elaborated a new host material based on blocks and construction of 9H-carbazole being incorporated the indole block [3,2,1-jk] carbazole (ICz).

The device elaborated by the authors is represented in Fig. 30, where it is possible to notice that it has the following structure for the red light emitter, ITO/MoO3/TAPC/EML (host material: $Ir(MDQ_2(acac))$/Bphen/LiF/Al, where TAPC corresponds to the transport material and holes, $Ir(MDQ_2(acac))$ to the

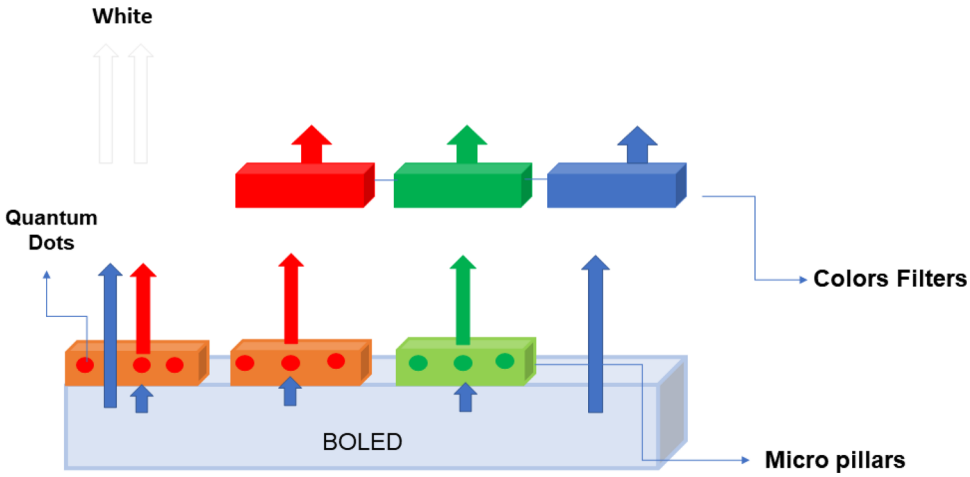

Fig. 29 Schematic representation of the device consisting of a blue pumping emitter, a color filter, and quantum dots on micropillars (adapted from [144])

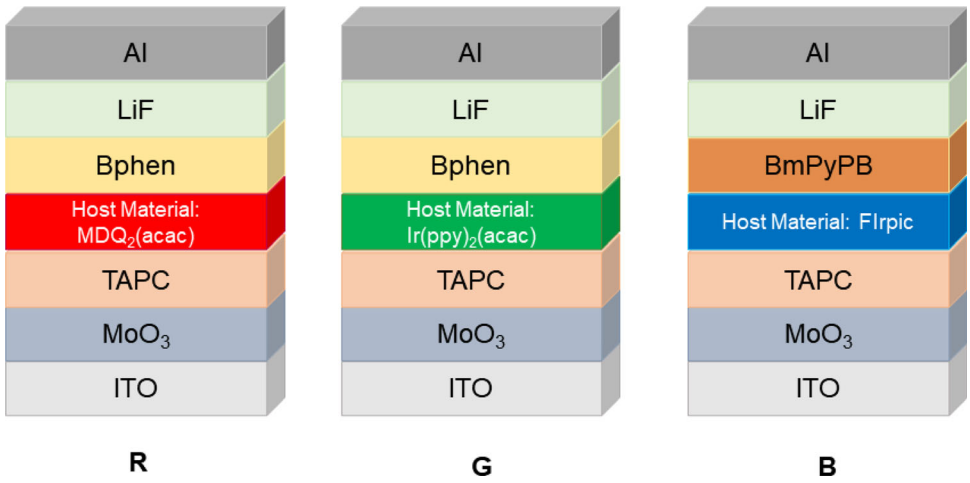

Fig. 30 Schematic representation of devices made with phosphorescent RGB light-emitting components used as host material based on ICz (adapted from [145])

red emitter and Bphen electron transport material and to block holes. For the green light-emitting device, the structure is very close to that of the red emitter, with the only difference being the green emitter in the emission layer, consisting of the host material and $Ir(ppy)_2(acac)$ (ITO/ MoO_3/TAPC/ EML (host material: $Ir(ppy_2(acac)$/Bphen)/LiF/Al. Finally, the blue light emission device, in addition to having a blue emission compound in the FIrpic EML, the electron transport layer and the blocking of holes that previously belonged to Bphen was replaced by BmPyPB (ITO/MoO_3/TAPC/EML (host material:FIrpic)/BmPyPB/LiF/Al), by this component has higher triplet energy and therefore has a greater capacity to confine the excitons the emitting material.

The work developed aims to control excimers' formation utilizing the host materials' molecular design based on ICz. Thus, structural changes in these hosts' building blocks have been proposed to mitigate possible intermolecular interactions. Thus, the molecule's symmetry was reduced, changing the substitution position of the 9H-carbazole block from position 2 to 5 (Fig. 31).

The host materials' molecular design strategy proved to be promising since the external quantum efficiencies for green emitters were increased from 15 to 20% when the emitter was replaced in position C5 instead of C2. Such a change in the efficiency data is associated with an efficient containment of the phosphorescent emitters' excitons. As for the blue-emitting devices, where the modified host 5CzICz was used, the quantum efficiency of 18% was obtained.

8 RGB type light-emitting polymers

As the present review seeks to develop an active polymeric layer, the electroluminescent polymers that could be used for this purpose are evaluated,

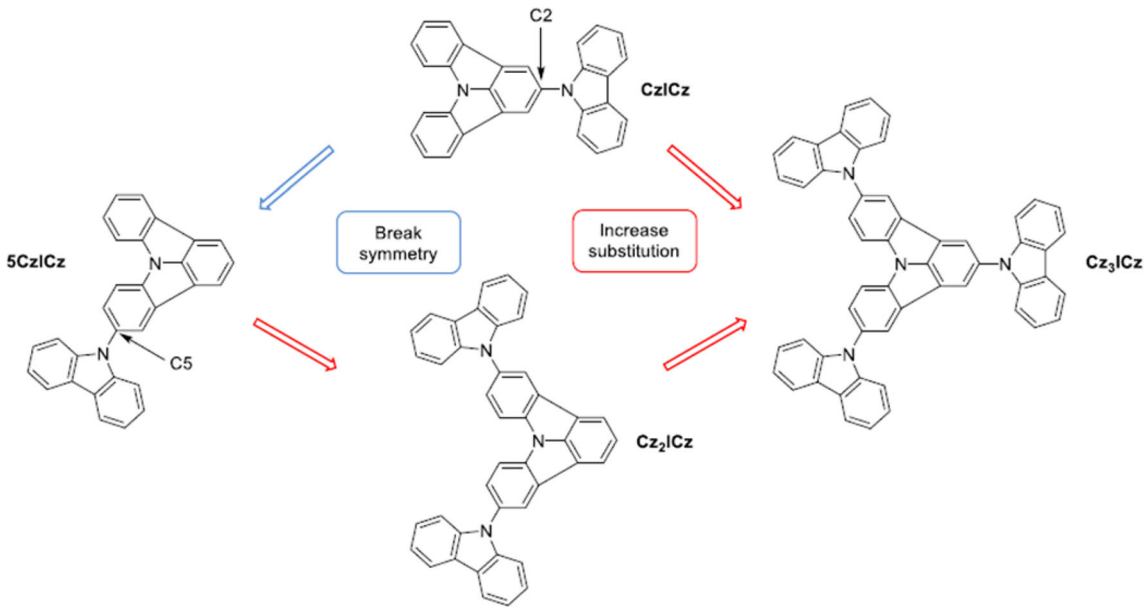

Fig. 31 Design of host materials based on ICz and the proposed structural modifications [145]

Fig. 32 Structure of fluorene derivatives

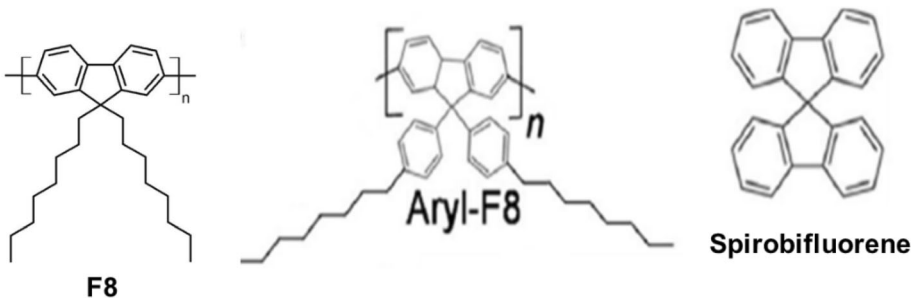

which are the ones that emit in the RGB bands, where different combinations used would reveal white light. Thus, in later items, polymers that have such property are discussed.

8.1 Blue light-emitting polymers

Usually, the polymers emitting in this range are based on para-phenylene vinylene (PPV) and fluorene (PF) monomers. However, the basic structure of PPV has not been successful in generating useful blue emissions due to its propensity to degrade oxidatively in the presence of air and light [146]. Thus, PF is preferentially used against phosphorescent materials due to their ease of synthesis. They present a high quantum photoluminescence yield (PLQY) and offer the stability of the elaborated device [52, 72, 147]. The most used PFs are poly(9,9-dihexylfluorene) (F8), aryl-F8, and spirobifluorene, whose structures are in Fig. 32.

Light-emitting polymers based on polyfluorenes can be obtained through the Suzuki coupling reaction (Fig. 33), a carbon–carbon coupling method using simple bonds based on a boronic ester or acid, and a halogenated monomer (brominated compound), using a palladium-containing catalyst. If the dibromated and diboronated aryls are the same, the coupling has a homopolymer as a product, and if they are different, the product will be an alternating copolymer [146, 148].

It is worth mentioning that the polymerization occurs to respect the catalyst's stoichiometry, which is available at each cycle. However, polyfluorenes suffer from defects arising from the low energy level of HOMO and with unbalanced mobility of charge carriers, which results in low electroluminescence (EL) performance. Thus, strategies are developed in

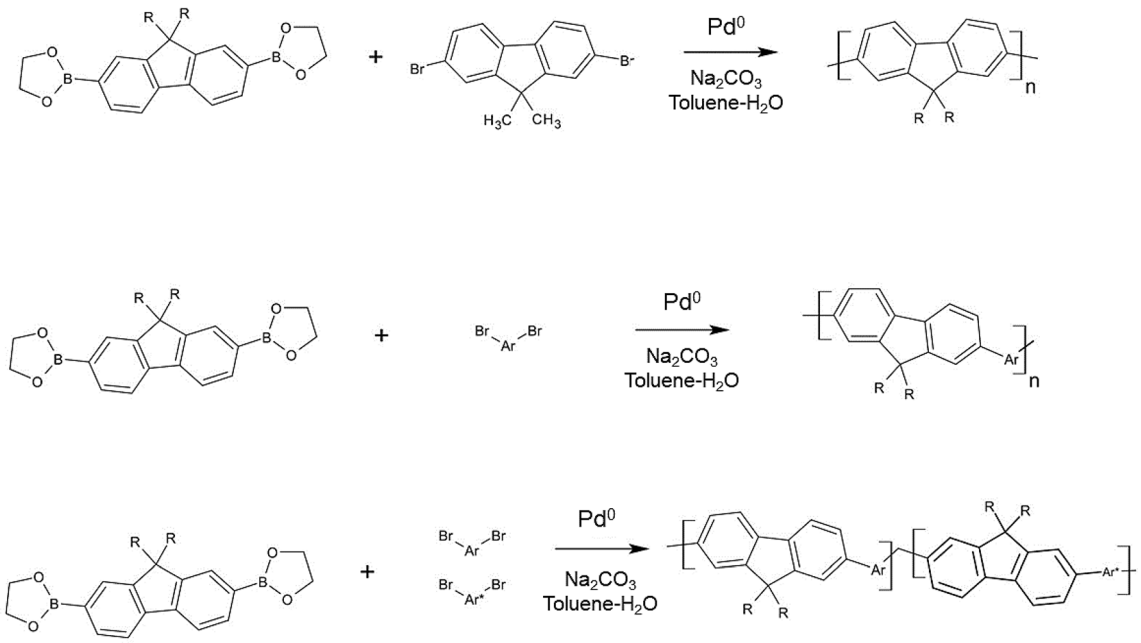

Fig. 33 Schematic representation of the Suzuki synthesis of fluorene-based polymers

order to mitigate such problems [149], such as, for example, incorporating a charge transport unit and/or a chromophore in the polyfluorene structure.

Thus, there are numerous possibilities for chromophores that can be incorporated into the fluorene polymer backbone, some of which are shown in Fig. 34.

The copolymers formed show high photoluminescence, and the bandgap defines the emitted wavelength, which can be correlated with the extent of the displacement of comonomers in the polymer chain.

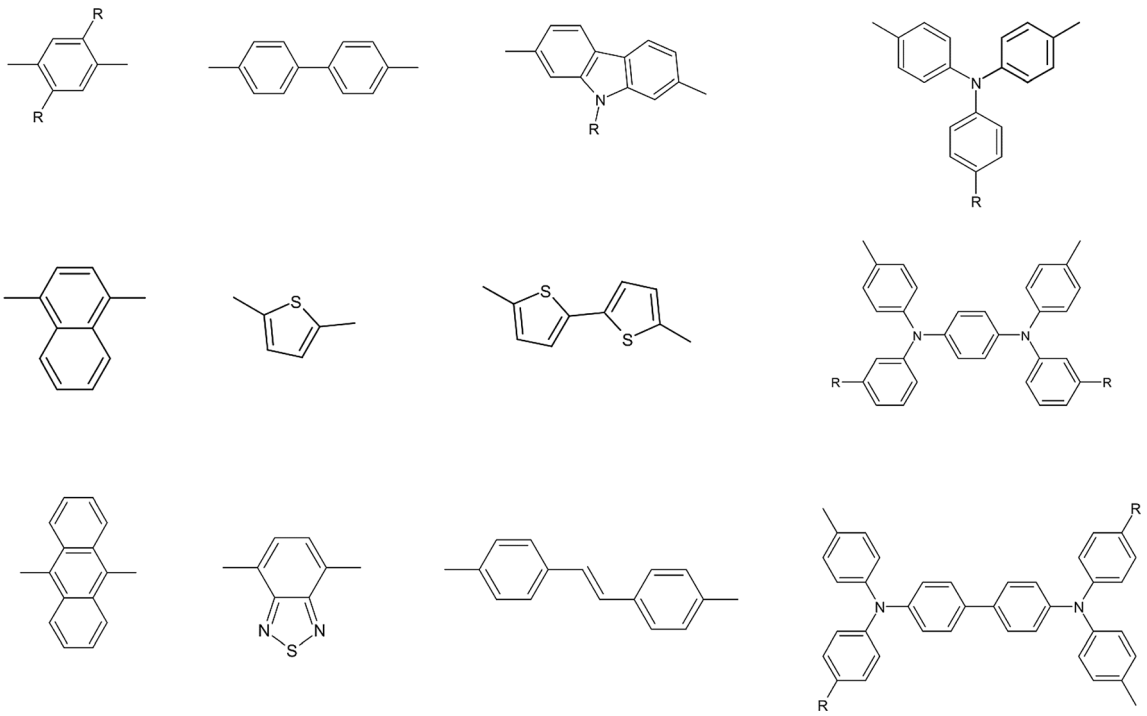

Fig. 34 Example of monomers that can be used for fluorene copolymers

For example, the thiophene copolymer emits blue-green light, while the 2,2′-bithiophene copolymer emits yellow light; that is, the conjugation's extent influences the emission that the polymer may have [146, 150].

In this way, fluorene-based copolymers can be designed based on the choice of comonomers in order to acquire balanced transport properties for carriers, with varying emission [141, 151].

Ma et al. [54] developed a device where the emitting layer (Fig. 35) consists of a fluorene copolymer with SO units, a component with the potential to remove electrons and which helps in emitting bright blue light in conjugated polymers of high performance [147, 152]. The insertion of these units, which have electron deficiency in the backbone of copolymers, facilitates the injection and transport of electrons and makes it difficult to inject and transport holes, which provides a better balance of carriers in the device for consequent recombination in the active layer. Thus, the developed architecture of the poly[9,9-bis(4-(2-ethylhexyloxy)phenyl) fluorene-co-dibenzothiophene-S,S′-dioxide) copolymer (PPF-SO20) and the insertion of a double hole transport layer (HTLs) consisting of PVK and a copolymer of indenofluorene-*co*-triphenylamine (X-IFTPA) leads to an injection of carriers in the form of a cascade up to the blue light emitter (PPF-SO20); such devices significantly increase the maximum luminous efficiency (LE_{max}), whose value reached by the elaborated device was 7.67 cd/A, the highest value obtained for devices based on X-IFTPA or PVK as a hole carrier layer.

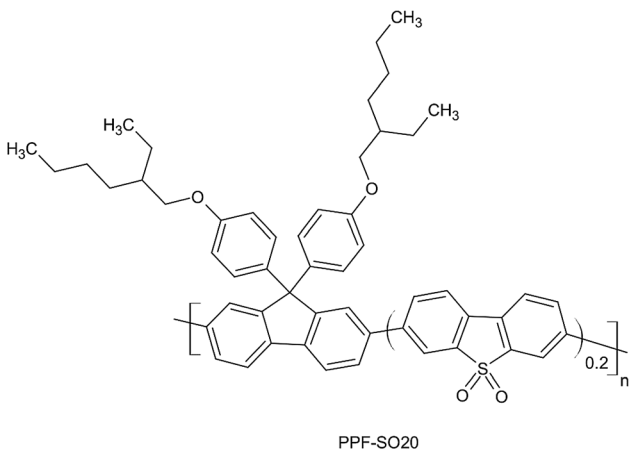

Fig. 35 Structure of the fluorene copolymer with SO20

Peng et al. [153] developed a series of polymers based on poly(9,9-dioctylfluorene) (PFO), in which blue styrylene amine chromophores were inserted (E)-4-(*t*-butyl)-*N*-phenyl-*N*-(4-styrylphenyl)- aniline (DV) (Fig. 36).

The styrylene amine derivatives (4,4′-4,4′-*bis*[2-(4-(*N*,*N*-diphenylamino)phenyl) vinyl]-biphenyl (DPAVBi) and 4,4′-*bis*((E)-2-(9-ethyl-9H-carbazol-3-yl)vinyl)-1,1′-biphenyl (BCzVBi)) have high hole mobility and high PLQY values and have been widely used as high-fluorescent blue dopants efficiency in thermally evaporated light-emitting diodes. It can be seen in Fig. 36 that the monomers can be prepared in three stages with good yields, which is favorable for the expansion of the projected polymers. When adjusting the molar proportions of the chromophores of F-$Bpin_2$:F-Br_2:TD-Br_2:DV-Br_2 in the ratios of 50:48:2:0, 50:48:0:2, 50:46:2:2, and 50:40:5:5, polymers PF-TD_2, PF-DV_2, PF-TD_2DV_2, and PF-TD_5-DV_5 were obtained. The latter was the one that reached the highest luminous efficiency value, which corresponds to 5.47 cd A^{-1}, with CIE coordinates of (0.15, 0.14) [153].

As noted throughout the discussion in this session, blue light emitters' development is a challenge since they are less efficient than red and green emitters. In this way, different technologies are developed to work around this problem.

Lee et al. [154] reported a study on material selection and operating principles to achieve efficient blue emission devices. Among the emission mechanisms, there is the use of phosphorescent materials, triplet–triplet fluorescence (TTF), thermally activated delayed fluorescence (TADF), or hybridized emission and charge transfer (HLCT). The differences between the mechanisms are related to the energy states. In the fluorescence mechanism, it is possible to reach up to 25% of the quantum efficiency. After the electrical pumping, the phosphorescence mechanism, 25% of the singlet excites, and 75% of the triplets are formed. Singlet excites via intersystem intersection (ISC) are brought to the triplet state. In this way, it is possible to achieve 100% internal quantum efficiency. The mechanism is known as triplet–triplet annihilation (TTA); two triplets can merge into a light emission singlet. Finally, the thermally activated delayed fluorescence (TADF) mechanism reduces the energy difference between singlet and triplet states, where triplet excitons can be converted to singlet employing reverse intersystem crossing (RISC). Therefore, the

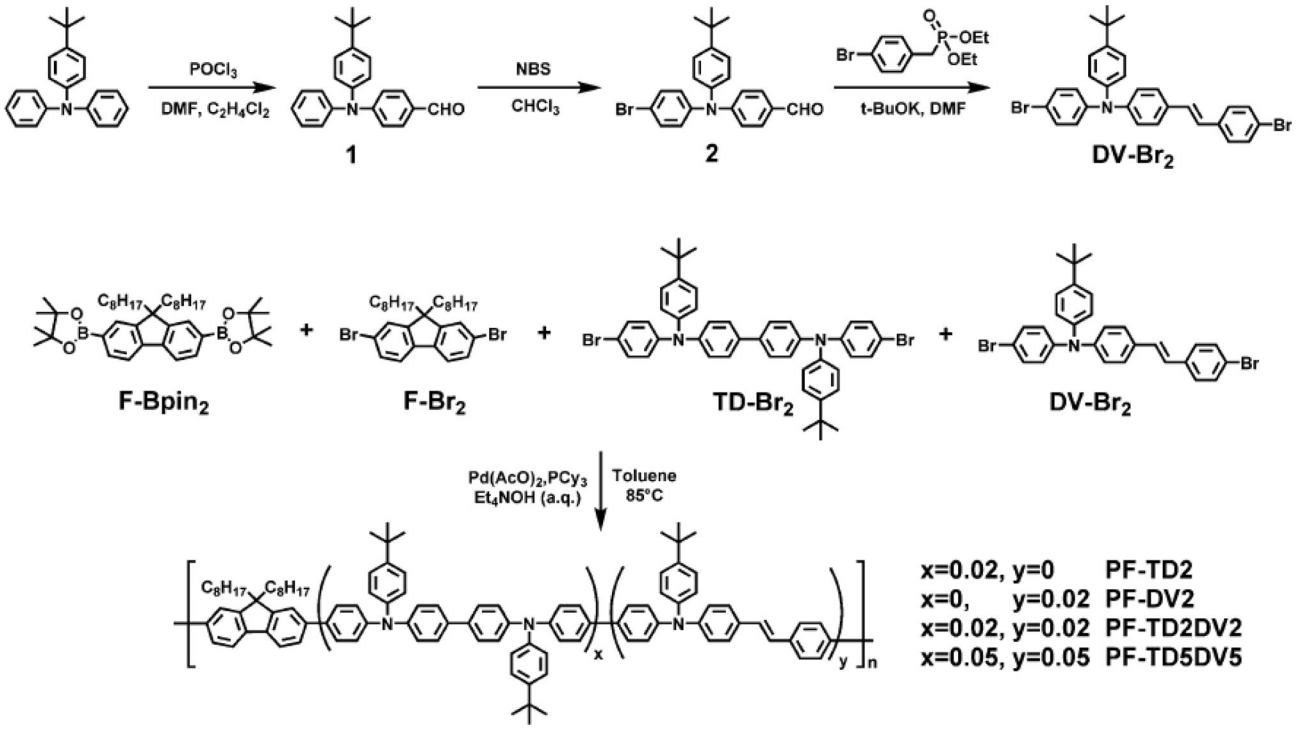

Fig. 36 Chemical structures and synthetic routes for monomers and polymers [153]

choice of the emission mechanism, as well as the components of the device, influence the efficiency that it can present. Thus, in devices that employ the triple-triple-annihilation mechanism, the authors mention the use of doping materials derived from anthracene to obtain deep blue emission, which is a twisted configuration material with a bisanthracene core that revealed a reduction in conjugation that allowed the electron donor employed, methoxy (OMe) and the cyan acceptor (CN) when connected to avoid the bathochromic effect, in which the wavelength shift occurs due to the effect of the solvent or a substituting group. Thus, when attaching the butoxyphenyl group to the anthracene nucleus, the quantum photoluminescence yield (PLQY) was increased, demonstrating that the TTA process was suitable for obtaining deep blue light.

For devices that employ the phosphorescence mechanism, the complexes used, as well as the materials to be deposited by the carrier transport layer, are important, as they affect the performance of the blue PHOLED device produced. Therefore, the authors report that several platinum complexes show promising results by substituting the already known Iridium complexes.

For the TADF mechanism for blue light emitters, it is proposed to employ two strong electron donors, having, for example, acridan. A weak electron acceptor, such as diphenylsulfone, thus developing the DMAC-DPS. However, the material has a short lifespan, and modifications are proposed to transpose this response and replace the components with carbazole and cyan as weak electron donors and are strong, accepting fractions, thus achieving efficient blue emission.

In this way, it is possible to improve the efficiency of the devices using the mechanisms mentioned.

8.2 Green light-emitting polymers

As mentioned, the synthesis of fluorene copolymers has been gaining prominence in recent research for reducing the problems of stability and low efficiency of maximum luminosity and, therefore, for emitting green light, such a group of polymers is also employed. So far, several models have been proposed to explain the origin of the green emission. Nevertheless, there is still nothing conclusive as to the nature of it. Initially, the green emission of polyfluorenes is attributed to the agglomeration of carriers based on previous observations about poly(*p*-

phenylene); however, later, it was attributed to the emission of excimers (excited dimers in which emission of light occurs) formed by the most planar fluorene and produced by photo/electro-oxidation at position 9 of the fluorene unit [155].

However, a new hypothesis was raised, stating that the polyfluorene chain's isolated defects can cause green light emission. Such defects can be formed during polymerization or later, using thermal oxidation or photo-oxidation of the formed polymeric films. This hypothesis's main indication was the green emission band's observation in diluted solutions of fluorenone oligomers, polymers, and copolymers. The lack of any significant dependence on the concentration and vibrational structure of the emission band at low temperatures [156]. Results of time-dependent electroluminescence spectroscopy reveal that the green emission band's contribution is greater than the blue when the delay time is increased. This phenomenon is attributed to the delayed recombination of charge carriers in the fluorenone defects, which act as electrical traps [157].

Also, some theoretical studies on fluorenone-containing oligomers demonstrate that green emission originates from efficient energy transfer and the location of excitons in their low-energy units. Thus, the incorporation of defects in the fluorene structure culminates in the extinction of the blue emission; however, it helps in the efficient emission of green light in electroluminescent materials [158, 159].

Among the fluorene copolymers with the best PLQY, poly(9,9-dioctylfluorene-co-benzothiadiazole) (F8BT) (Fig. 37) stands out for presenting high stability and good charge transport properties [160].

As mentioned, polyfluorenes are materials that allow the modification of light emission by the insertion of electron-accepting groups, as in the case of benzothiadiazole and side-chain engineering [161, 162]. Thus, the F8BT conjugated polymer is an efficient emitter of green light, with a photoluminescence efficiency of 50 to 60% in solid films. In addition, it exhibits a relatively high electronic affinity, equivalent to 3.3 eV, and a great ionization potential (5.9 eV) [163]. Thus, many studies report using this group to assist in transporting electrons in organic light-emitting diodes.

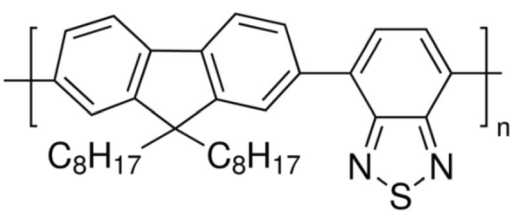

Fig. 37 Structure of poly (9,9-dioctylfluorene-co-benzothiadiazole)

Mucur et al. [88] developed fluorene-based polymers named SF5 and SF6, which were produced by the Suzuki coupling reaction, and their structures are shown in Fig. 38.

The devices with SF5 and SF6 revealed maximum luminance of 3165 and 5272 cd m^{-2}, the maximum luminous efficiency of 1.20 and 1.28 cd A^{-1}, and activation voltage of 7.5 and 8.2 V, respectively. Both polymers showed the same electroluminescence characteristic, with a wavelength around 545 nm, the visible spectrum's green region. The OLEDs' emission color produced with these polymers under the operating voltage of 13 V can be seen in Fig. 39.

Ma et al. [82], carrying out a study on the processing in orthogonal solutions of fluorene derivatives, developed a device in which the active layer was composed of a green emitter, PPF-SO15-BT1 (Fig. 40). It comprises an S, S-dioxidibenzothiophene fraction (15 mol%) in the main chain, phenyl groups substituted by alkoxy in the side groups, and an extra portion 2,1,3-benzothiadiazole (BT, 1 mol%).

Polymer PPF-SO15-BT1, which has a portion of benzothiadiazole, has very similar energy levels (HOMO/LUMO = − 5.89/–2.56 eV) to that of the polymer in the absence of BT (PPF-SO15) (HOMO/LUMO = − 5.94/-2.53 eV), since the molar ratio of this component is very small and, therefore, the difference is not detected by the cyclic voltammetry technique. However, by employing a suitable hole carrier layer, in this case, the poly(9,9-dioctylfluorene) functionalized with a triphenylamine derivative (PFO-TF), an increase in the bonding tension (V_{on}) of 0.2 V was observed, compared to the same device without adding an HTL. The electroluminescence and photoluminescence reached values of 22.27 cd A^{-1} and 18.41 lm W^{-1}, respectively. In this way, it is known that such a copolymer is a promising material for HTL in green light-emitting devices.

8.3 Red light-emitting polymers

One of the most used polymers for the emission of red light is the poly[2-methoxy-5-(2-ethylhexyloxy)-1,4-phenylenevinylene] (MEH-PPV), in which its

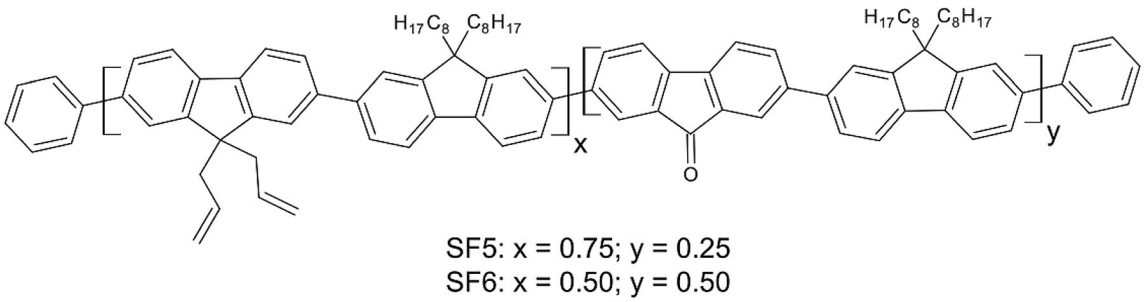

Fig. 38 Structure of SF5 and SF6 polymers

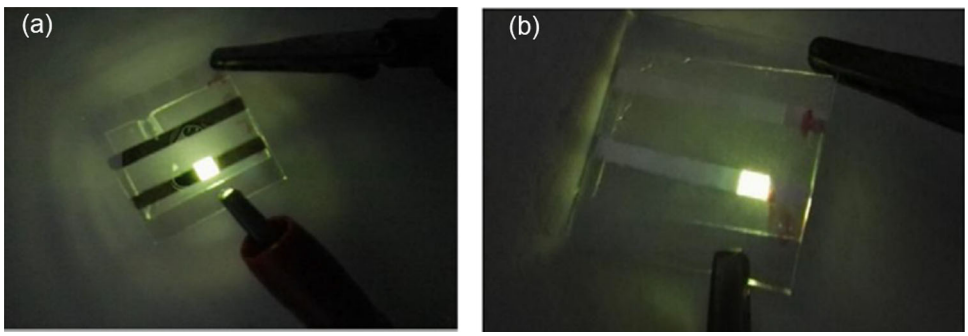

Fig. 39 Light emission from OLEDs with a light-emitting layer **a** SF5 polymers and **b** SF6 [88]

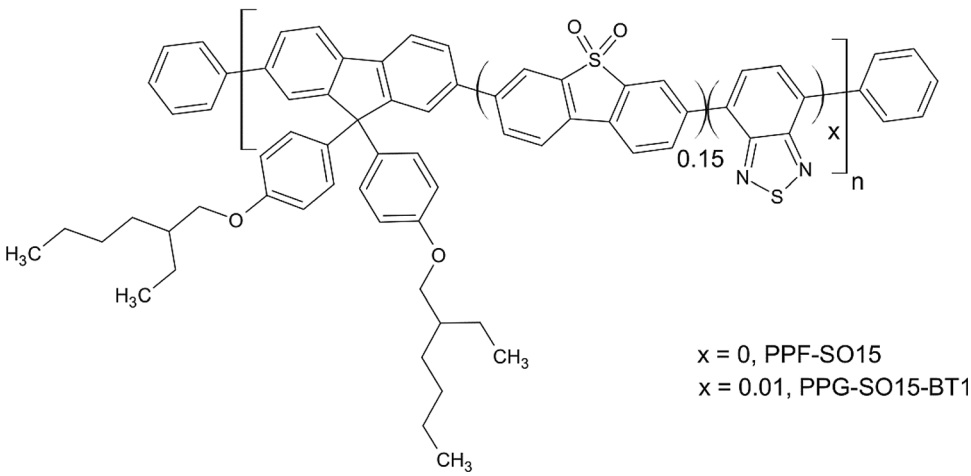

Fig. 40 Structure of the green light-emitting layer (*x*: PPF-SO15; PPF-SO15-BT1)

emission is attributed to chromophore units and interactions between them, possibly resulting in excimers or aggregates. This fact expresses that the electronic coupling close to the chromophores is not large enough to relocate the excitation, which results in regions of a high density of chromophores in the structure. Consequently, there is an increase in the conjugation length [164].

However, PLEDs devices based on red emission have lower purity and efficiency than green emission and demonstrate a low PLQY due to strong intermolecular interactions that occur through dipole–dipole coupling and/or π–π stacking, which leads to the extinction of the exciton. Thus, many efforts are made to change this scenario [165, 166]. Among the alternatives adopted, there is the insertion of red light-emitting fractions with narrowband intervals, such as those derived from 2,1,3-benzothiadiazole and 2,1,3-benzoselendiazole in the main chain, in the side chain, or still in terminal polymer groups [167, 168]. Such alternatives reduce the content of red fluorophores, thus, make impossible the effect of attenuation of the concentration that arises from the dipole–dipole interactions and/or stacking π-π [169, 170].

Zaumseil et al. [170] report an alternative for the more efficient emission of red light, obtaining control of the optical and electrical properties of polymers based on poly(octyl fluorene) (PFO). Such control is performed through chemical modification provided by the insertion of comonomers, such as 4,7-*bis* (2)-thienyl)-2,1,3-benzothiadiazole (TBT) in the PFO backbone.

Liu et al. [166] performed the synthesis of a conjugated emitter polymer in red based on triphenylaminasilol-carbazole-fluorene (PFO-Cz-TPATST), shown in Fig. 41.

Such a strategy was adopted in order to combine the properties of the components of the terpolymer since the materials based on polyfluorene are used for revealing high photoluminescence and electroluminescence efficiency, excellent thermal stability, and good solubility in organic solvents, which facilitates their processing. However, they present a high barrier to the injection of holes due to lower HOMO levels, around -5.7 eV. For this reason, polycarbazole (PCz) was chosen, which exhibits adequate hole injection with energy levels close to the anode. The triphenylamine silol unit (TPA) was incorporated in positions 3, 4 of the PCz skeleton. Based on this choice, it can be seen that the hole injection barrier of polyfluorenes (PF) can be exceeded by using carbazole as a comonomer. Therefore, it has been shown that the insertion of red fluorophores into the skeleton of the fluorene copolymer with carbazole is an effective way to achieve efficient red light-emitting devices [166, 171, 172].

Nimith et al. [173] developed a device with few layers using MEH-PPV as an active layer mixed with benzothiadiazole (BT). This small molecule has electron deficiency, motivated by the balance of carriers in the device, to achieve better photoluminescence efficiencies. In a less complex structure, the lower drive voltage can be achieved, and the useful life of these devices can be increased.

The insertion of benzodiatiazole proved to be a good alternative since this component does not affect MEH-PPV emission. However, it induces charge transport in the polymer, presenting a predominant peak at 569 nm and a shoulder at 610 nm (Fig. 42) in both systems proposed (without and adding benzodiathiazole).

Lee et al. [165] developed a highly efficient polymeric red-light emitting device via Förster resonance energy transfer (FRET) based on homogeneous mixtures of polymers with the same polyfluorene backbone. The polymers employed were poly(9,9′-dioctylfluorene-co-2,1,3-benzothiadiazole) (F8BT) and poly[9,9′-dioctylfluorene-co-(4,7-bis(4-hexyl-2-thienyl)-2,1,3-benzothiadiazole)] (F8TBT) (Fig. 43). The approach performed revealed the desired emission with CIE coordinate (0.62, 0.38) and a light efficiency of 7.14 cd A^{-1}.

When modifying the electron transport layer consisting of zinc oxide (ZnO) with a cationic conjugated polyelectrolyte, the poly(9,9′-*bis*(6″-*N*,*N*,*N*-trimethylammoniumhexyl)fluorene-*alt*-phenylene) with bromide counter-ions (FPQ-Br) for efficient electron transport and blocking of holes in inverted PLEDs, high efficiencies of pure red emission were achieved with a maximum luminance of 26,400 cd m^{-2} and a voltage luminance of 12.8 V. So far, the efficiency obtained by the authors is one of the highest reported for red emission.

Kim et al. [174] report the progress of TADF fluorescent red emitters; these present themselves as an alternative to achieve external quantum efficiencies greater than 20% that were reported until then, which motivated many research groups to develop work on the design of red OLED TADF materials [175, 176]. The red TADF emitters require little singlet energy to

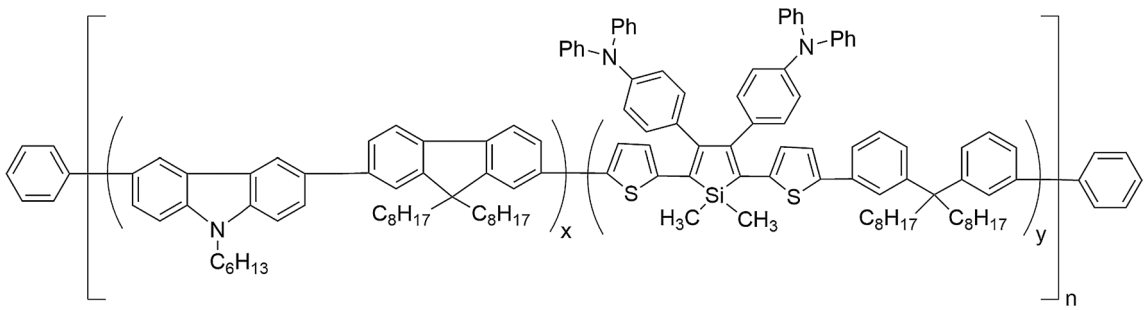

Fig. 41 Structure of PFO-Cz-TPATST terpolymer [166]

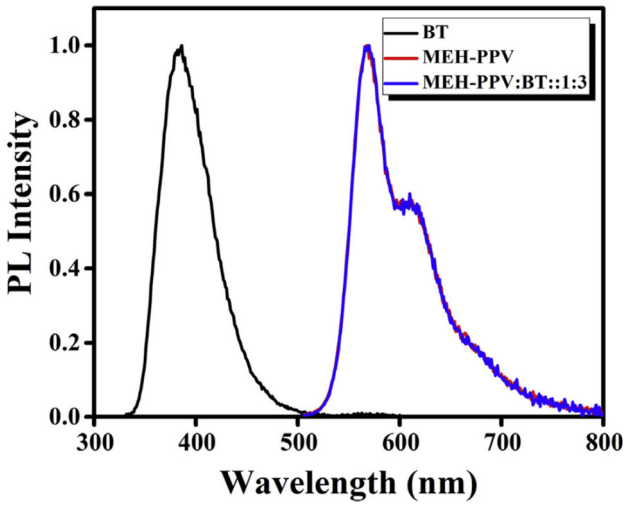

Fig. 42 Normalized fluorescence spectra of MEH-PPV, BT, and MEH-PPV:BT (1:3 mass ratio) solutions in DCB solvent

emit light, achieved by intensifying the charge transfer (CT) through adjustment adjusted by the strength of the donor and acceptor components, which in both cases must be strong to induce a small gap between the HOMO–LUMO orbitals since strong donors provide shallow HOMO and strong acceptors provide deep LUMO. Thus, some strong donor groups can be employed to construct TADF emitting polymers of red light; these are triphenylamine, t-butylated triphenylamine, dimethylacridane, and diphenylacridane, whereas acceptors are based on diphenyltriazine, quinoxaline, dibenzophenazine, cyanobenzazine, benzophenone, and benzothiadiazole.

Bearing in mind that the majority of red chromophores made up of donors and acceptors are susceptible to stacking, dipole–dipole aggregation, and tempering [177], Sudyoadsuk et al. [178] have developed saturated red emitters based on benzothiadiazole for non-doped electroluminescent devices that can be processed in solution. The emitting component structure has a benzothiadiazole core with two isomeric n-hexylthiophenes to form the conjugated skeleton. To this structure (Fig. 44), triphenylamine groups (electron donors) were added at different positions in the thiophene chain, forming the donor-type molecular structure—red emission acceptor.

With the alternative devised by the authors (the insertion of triphenylamine fractions in the thiophene ring), it was possible to improve the performance of the device, with emphasis on the one composed of BTZ2, with a maximum EQE of 4.15% and maximum luminance of 6842 cd m^{-2}. It is worth mentioning that the data obtained refer to an undoped material.

9 Non-conventional electrodes in light-emitting devices

Usually, transparent electrodes are used in light-emitting devices to allow the passage of light. In addition to having about 80% transmittance in the visible region and specific resistance [179–181] around the most cited materials, there is doped indium oxide tin (ITO) [182]; however new materials have been considered for this purpose.

Because of the variety of materials that can be used, Song et al. [181] developed a study about a conductive antimony transparent electrode; this has a work function of 5.1 eV, compared to 4.7 eV of ITO. The elaborated PLED device is shown in Fig. 45.

The device recorded maximum brightness and max efficiency of 3673 cd m^{-2} and 1.03 cd A^{-1}, respectively (Fig. 46). Moreover, in terms of the CIE coordinate, it presented the same coordinates as the device with the anode ITO; therefore, a possible substitute, with the advantage of wet processing.

As ITO is a rigid material, it makes it difficult to use in flexible devices. Thus, thin films of carbon

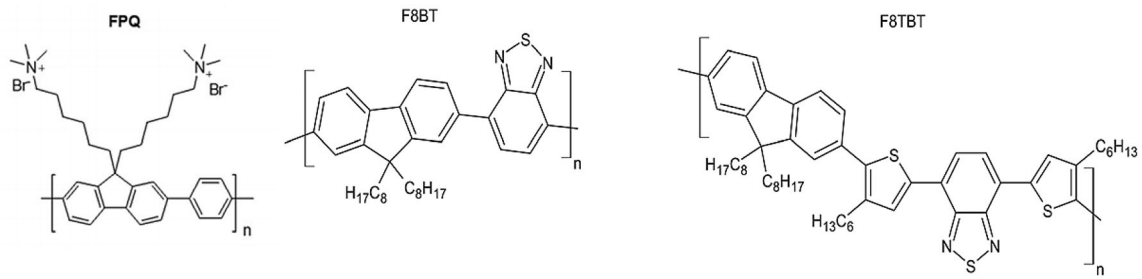

Fig. 43 Chemical structure of F8BT and F8TBT polymers

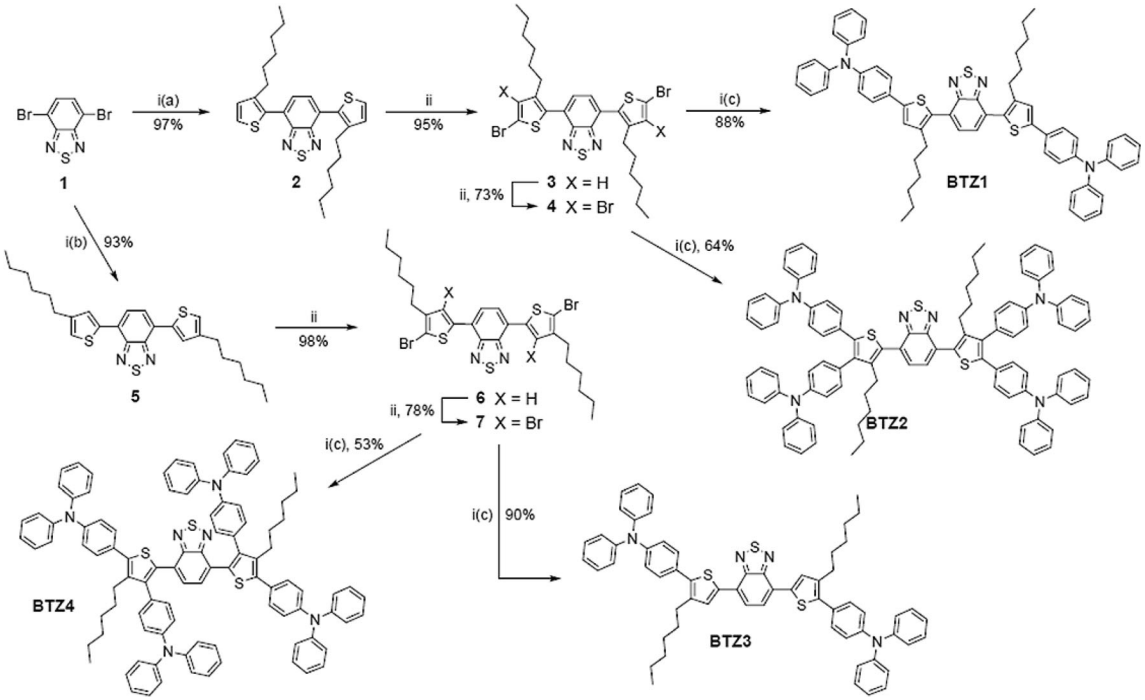

Fig. 44 Synthesis of the red light-emitting component based on benzothiadiazole and thiophene [178]

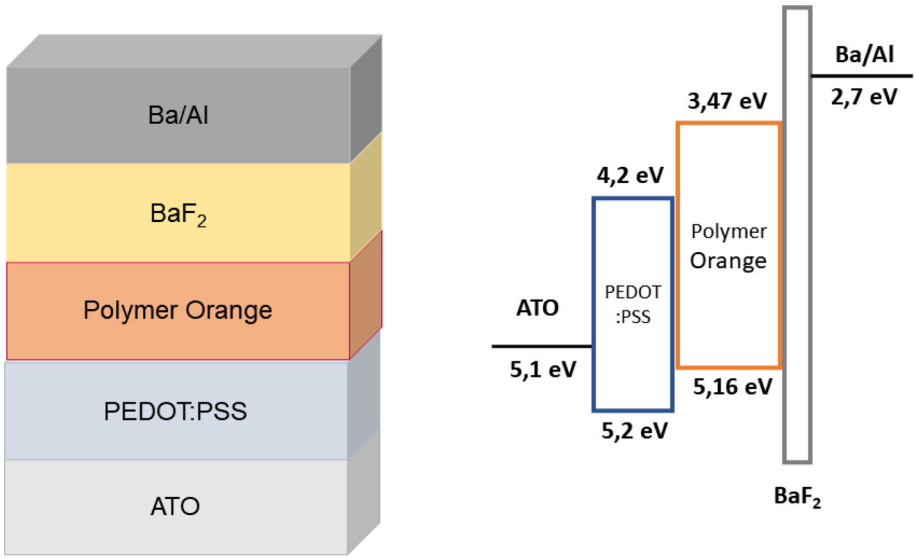

Fig. 45 Schematic representation of the device's structure using an ATO electrode and energy levels (adapted from [181])

nanotubes (SWNT) have been studied to replace ITO since SWNTs have low sheet resistance and high transmission, coming from interconnected nanotube networks. Another electrode also studied is silver nanofilms (AgNW). These are reported by Yu et al. [183] when developing flexible silver nanowire electrodes for light-emitting polymeric diodes with shape memory. The developed device is shown in Fig. 46, this consisted of a polyacrylate substrate, anode of silver nanowires (AgNW), a hole-carrying layer of PEDOT:PSS, the emitting layer of alkoxyphenyl substituted yellow emissive poly (1,4-phenylene vinylene) (SY-PPV), an electron carrier layer of cesium fluoride (CsF) and an aluminum cathode (Al) were placed on this layer.

It can be noted that the method for obtaining thin layers of silver nanowires is relatively simple and can be used in flexible substrates, in this case, a transparent cross-linked polyacrylate substrate, presenting low surface resistance and high solvent resistivity,

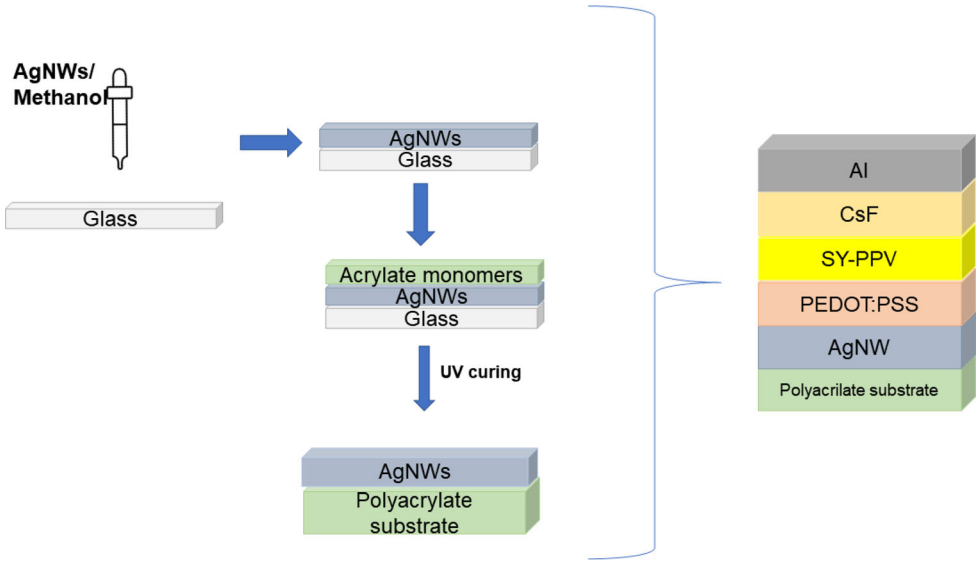

Fig. 46 Schematic representation of the polymeric light-emitting device that has silver nanowires (AgNW) anode (adapted from [183])

which allows its use in processing PLED devices, which are usually processed in solution.

10 Conclusion and outlook

From this literature review, it is possible to verify that developing a new material and construction processes for a PLED device are complex since many factors can affect the light-emitting diode's performance. However, it is noted that there are countless works developed looking for alternatives to obtain greater efficiency, architecting the structure of the polymers employed, either by doping, by copolymerization or by the development of polymer blends, as well as by modifying the architecture, by using different solvents for deposition or by changing the method of deposition. All are strategies to better balance charges in the active layer and control the charge bearers' mobility through the subsequent layers.

For the application in solid-state lighting, there is a need for improvements in luminous efficiency. These are achieved when there is a layered architecture design with less resistive structure. In other words, the choice of the injector layers of holes and electrons, as well as the energy of the molecular levels of the components, are important for the efficient formation of the excitons and, consequently, of the light emitted from the white light device.

Acknowledgements

The authors of this article thank the Brazilian support agencies Coordination for the Improvement of Higher Education Personnel (CAPES), The Brazilian National Council for Scientific and Technological Development (CNPq), and Carlos Chagas Filho Foundation for Research Support of the State of Rio de Janeiro (FAPERJ) for the financing.

References

1. J.H. Burroughes, C.A. Jones, R.H. Friend, New semiconductor device physics in polymer diodes and transistors. Nature **335**, 137–141 (1988). https://doi.org/10.1038/335137a0
2. S.C. Rasmussen, The path to conductive polyacetylene. Bull. Hist. Chem. **39**, 64–72 (2014)
3. Q. Burlingame, C. Coburn, X. Che, A. Panda, Y. Qu, S.R. Forrest, Centimetre-scale electron diffusion in photoactive organic heterostructures. Nature **554**, 77–80 (2018). https://doi.org/10.1038/nature25148
4. J.H. Burroughes, D.D.C. Bradley, A.R. Brown, R.N. Marks, K. Mackay, R.H. Friend, P.L. Burns, A.B. Holmes, Light-emitting diodes based on conjugated polymers. Nature **347**, 539–541 (1990). https://doi.org/10.1038/347539a0
5. H. Huang, L. Yang, A. Facchetti, T.J. Marks, Organic and polymeric semiconductors enhanced by noncovalent conformational locks. Chem. Rev. **117**, 10291–10318 (2017). https://doi.org/10.1021/acs.chemrev.7b00084

6. C. Wang, H. Dong, L. Jiang, W. Hu, Organic semiconductor crystals. Chem. Soc. Rev. **47**, 422–500 (2018). https://doi.org/10.1039/C7CS00490G
7. R. Coehoorn, W.F. Pasveer, P.A. Bobbert, M.A.J. Michels, Charge-carrier concentration dependence of the hopping mobility in organic materials with Gaussian disorder. Phys. Rev. B (2005). https://doi.org/10.1103/PhysRevB.72.155206
8. S. Fratini, M. Nikolka, A. Salleo, G. Schweicher, H. Sirringhaus, Charge transport in high-mobility conjugated polymers and molecular semiconductors. Nat. Mater. **19**, 491–502 (2020). https://doi.org/10.1038/s41563-020-0647-2
9. W. Ji, J. Zhao, Z. Sun, W. Xie, High-color-rendering flexible top-emitting warm-white organic light emitting diode with a transparent multilayer cathode. Org. Electron. **12**, 1137–1141 (2011). https://doi.org/10.1016/j.orgel.2011.03.042
10. P. Freitag, S. Reineke, S. Olthof, M. Furno, B. Lüssem, K. Leo, White top-emitting organic light-emitting diodes with forward directed emission and high color quality. Org. Electron. **11**, 1676–1682 (2010). https://doi.org/10.1016/j.orgel.2010.07.017
11. H.F. Haneef, A.M. Zeidell, O.D. Jurchescu, Charge carrier traps in organic semiconductors: a review on the underlying physics and impact on electronic devices. J. Mater. Chem. C **8**, 759–787 (2020). https://doi.org/10.1039/c9tc05695e
12. W. Brütting, J. Frischeisen, T.D. Schmidt, B.J. Scholz, C. Mayr, Device efficiency of organic light-emitting diodes: Progress by improved light outcoupling. Phys. Status Solidi Appl. Mater. Sci. **210**, 44–65 (2013). https://doi.org/10.1002/pssa.201228320
13. F. Dumur, Carbazole-based polymers as hosts for solution-processed organic light-emitting diodes: simplicity, efficacy. Org. Electron. **25**, 345–361 (2015). https://doi.org/10.1016/j.orgel.2015.07.007
14. Q. Niu, R. Rohloff, G.-J.A.H. Wetzelaer, P.W.M. Blom, N.I. Crăciun, Hole trap formation in polymer light-emitting diodes under current stress. Nat. Mater. **17**, 557–562 (2018). https://doi.org/10.1038/s41563-018-0057-x
15. Y. Deng, J. Quinn, B. Sun, Y. He, J. Ellard, Y. Li, Thiophene-S, S-dioxidized indophenine (IDTO) based donor-acceptor polymers for n-channel organic thin film transistors. RSC Adv. **6**, 34849–34854 (2016). https://doi.org/10.1039/c6ra03221d
16. B. Meng, Y. Ren, J. Liu, F. Jäkle, L. Wang, p-π conjugated polymers based on stable triarylborane with n-type behavior in optoelectronic devices. Angew. Chem. **130**, 2205–2209 (2018). https://doi.org/10.1002/ange.201712598
17. T. Yamamoto, π-conjugated polymers with electronic and optical functionalities: preparation by organometallic polycondensation, properties, and applications. Macromol. Rapid Commun. **23**, 583–606 (2002). https://doi.org/10.1002/1521-3927(20020701)23:10/11%3c583::AID-MARC583%3e3.0.CO;2-I
18. R. Chesterfield, A. Johnson, C. Lang, M. Stainer, J. Ziebarth, Solution-coating technology for AMOLED displays. Inf. Disp. **27**(2011), 24–30 (1975). https://doi.org/10.1002/j.2637-496X.2011.tb00339.x
19. M. Goes, J.W. Verhoeven, H. Hofstraat, K. Brunner, OLED and PLED devices employing electrogenerated, intramolecular charge-transfer fluorescence. ChemPhysChem **4**, 349–358 (2003). https://doi.org/10.1002/cphc.200390061
20. I.C. Mota, M.F.V. Marques, Synthesis of polyvinylcarbazole/reduced graphite oxide-ZnO nanocomposites. Macromol. Symp. **383**, 1700081 (2019). https://doi.org/10.1002/masy.201700081
21. K. Bindumadhavan, S. Roy, S.K. Srivastava, B.B. Nayak, Synthesis and characterization of Poly(N-vinylcarbazole)/graphene nanocomposites. J. Nanosci. Nanotechnol. **15**, 3733–3742 (2015). https://doi.org/10.1166/jnn.2015.9485
22. A. Aashish, R. Ramakrishnan, J.D. Sudha, M. Sankaran, G. Krishnapriya, Self-assembled hybrid polyvinylcarbazole–titania nanotubes as an efficient photoanode for solar energy harvesting. Sol. Energy Mater. Sol. Cells **151**, 169–178 (2016). https://doi.org/10.1016/j.solmat.2016.03.007
23. T.H. Kim, H.K. Lee, O. Ok Park, B.D. Chin, S.H. Lee, J.K. Kim, White-light-emitting diodes based on iridium complexes via efficient energy transfer from a conjugated polymer. Adv. Funct. Mater. **16**, 611–617 (2006). https://doi.org/10.1002/adfm.200500621
24. A. Li, Y. Li, W. Cai, G. Zhou, Z. Chen, H. Wu, W.Y. Wong, W. Yang, J. Peng, Y. Cao, Realization of highly efficient white polymer light-emitting devices via interfacial energy transfer from poly(N-vinylcarbazole). Org. Electron. **11**, 529–534 (2010). https://doi.org/10.1016/j.orgel.2009.12.008
25. H. Zheng, Y. Zheng, J. Wang, J. Wang, G. Zhang, S. Zhang, M. Liu, J. Hu, Y. Li, Y. Hu, W. Zhang, Polymer light-emitting displays with printed cathodes. Surf. Coat. Technol. **358**, 228–234 (2019). https://doi.org/10.1016/j.surfcoat.2018.11.041
26. C. Amruth, M. Colella, J. Griffin, J. Kingsley, N. Scarratt, B. Luszczynska, J. Ulanski, Slot-die coating of double polymer layers for the fabrication of organic light emitting

diodes. Micromachines **10**, 53 (2019). https://doi.org/10.3390/mi10010053

27. N.E.A. Azhar, S.S. Shariffudin, S.A.H. Alrokayan, H.A. Khan, M. Rusop, *Annealing Temperature Effect on Electrical Properties of MEH-PPV Thin Film via Spin Coating Method* (Melville, AIP Publishing LLC, 2018), p. 020033. https://doi.org/10.1063/1.5036879
28. R. Colucci, M.H. Quadros, F.H. Feres, F.B. Maia, F.S. de Vicente, G.C. Faria, L.F. Santos, G. Gozzi, Cross-linked PEDOT: PSS as an alternative for low-cost solution-processed electronic devices. Synth. Met. **241**, 47–53 (2018). https://doi.org/10.1016/j.synthmet.2018.04.002
29. V. Vohra, T. Anzai, Molecular orientation of conjugated polymer chains in nanostructures and thin films: review of processes and application to optoelectronics. J. Nanomater. **2017**, 1–18 (2017). https://doi.org/10.1155/2017/3624750
30. X. Ban, A. Zhu, T. Zhang, Z. Tong, W. Jiang, Y. Sun, Highly efficient all-solution-processed fluorescent organic light-emitting diodes based on a novel self-host thermally activated delayed fluorescence emitter. ACS Appl. Mater. Interfaces **9**, 21900–21908 (2017). https://doi.org/10.1021/acsami.7b04146
31. B. Louis, S. Caubergh, P.-O. Larsson, Y. Tian, I.G. Scheblykin, Light and oxygen induce chain scission of conjugated polymers in solution. Phys. Chem. Chem. Phys. **20**, 1829–1837 (2018). https://doi.org/10.1039/C7CP07347J
32. S. Sato, S. Ohisa, Y. Hayashi, R. Sato, D. Yokoyama, T. Kato, M. Suzuki, T. Chiba, Y. Pu, J. Kido, Air-stable and high-performance solution-processed organic light-emitting devices based on hydrophobic polymeric ionic liquid carrier-injection layers. Adv. Mater. **30**, 1705915 (2018). https://doi.org/10.1002/adma.201705915
33. S.C. Mun, J.J. Park, Y.T. Park, D.Y. Kim, S.W. Lee, M. Cobos, S.J. Ye, C.W. Macosko, O. Ok Park, High electrical conductivity and oxygen barrier property of polymer-stabilized graphene thin films. Carbon N. Y. **125**, 492–499 (2017). https://doi.org/10.1016/j.carbon.2017.09.088
34. S. Scholz, D. Kondakov, B. Lüssem, K. Leo, Degradation mechanisms and reactions in organic light-emitting devices. Chem. Rev. **115**, 8449–8503 (2015). https://doi.org/10.1021/cr400704v
35. L. Ke, S.-J. Chua, K. Zhang, N. Yakovlev, Degradation and failure of organic light-emitting devices. Appl. Phys. Lett. **80**, 2195–2197 (2002). https://doi.org/10.1063/1.1464216
36. Y. Wu, Y. Liu, T. Emrick, T.P. Russell, Polymer design to promote low work function surfaces in organic electronics. Prog. Polym. Sci. **103**, 101222 (2020). https://doi.org/10.1016/j.progpolymsci.2020.101222
37. D.H. Lee, J.S. Choi, H. Chae, C.H. Chung, S.M. Cho, Highly efficient phosphorescent polymer OLEDs fabricated by screen printing. Displays **29**, 436–439 (2008). https://doi.org/10.1016/j.displa.2008.02.006
38. C. Feng, X. Zheng, R. Xu, Y. Zhou, H. Hu, T. Guo, J. Ding, L. Ying, F. Li, Highly efficient inkjet printed flexible organic light-emitting diodes with hybrid hole injection layer. Org. Electron. (2020). https://doi.org/10.1016/j.orgel.2020.105822
39. X. Liang, M. Tao, D. Wu, B. Yu, Y. Mi, Z. Cao, Z. Zhao, D. Chen, Multicolor AIE polymeric nanoparticles prepared via miniemulsion polymerization for inkjet printing. Dye. Pigments **177**, 108287 (2020). https://doi.org/10.1016/j.dyepig.2020.108287
40. T. Minshall, S. Seldon, D. Probert, Commercializing a disruptive technology based upon university ip through open innovation: a case study of cambridge display technology. Int. J. Innov. Technol. Manage. **04**, 225–239 (2007). https://doi.org/10.1142/S0219877007001107
41. J. Xu, F. Peng, Y. Yang, L. Hu, R. He, W. Yang, Y. Cao, Highly efficient inverted blue light-emitting diodes by thermal annealing and interfacial modification. Org. Electron. **49**, 1–8 (2017). https://doi.org/10.1016/j.orgel.2017.05.039
42. Y. Li, M. Kovačič, J. Westphalen, S. Oswald, Z. Ma, C. Hänisch, P.A. Will, L. Jiang, M. Junghaehnel, R. Scholz, S. Lenk, S. Reineke, Tailor-made nanostructures bridging chaos and order for highly efficient white organic light-emitting diodes. Nat. Commun. (2019). https://doi.org/10.1038/s41467-019-11032-z
43. L. Ying, C.-L. Ho, H. Wu, Y. Cao, W.-Y. Wong, White polymer light-emitting devices for solid-state lighting: materials, devices, and recent progress. Adv. Mater. **26**, 2459–2473 (2014). https://doi.org/10.1002/adma.201304784
44. M.C. Gather, A. Köhnen, A. Falcou, H. Becker, K. Meerholz, Solution-processed full-color polymer organic light-emitting diode displays fabricated by direct photolithography. Adv. Funct. Mater. **17**, 191–200 (2007). https://doi.org/10.1002/adfm.200600651
45. M.T. Bernius, M. Inbasekaran, J. O'Brien, W. Wu, Progress with light-emitting polymers. Adv. Mater. **12**, 1737–1750 (2000). https://doi.org/10.1002/1521-4095(200012)12:23%3c1737::AID-ADMA1737%3e3.0.CO;2-N
46. D. Costenaro, F. Carniato, G. Gatti, L. Marchese, C. Bisio, Organo-modified ZnO nanoparticles: tuning of the optical properties for PLED device fabrication. New J. Chem. **38**, 6205–6211 (2014). https://doi.org/10.1039/C4NJ01331J
47. C. Jiang, W. Yang, J. Peng, S. Xiao, Y. Cao, High-efficiency, saturated red-phosphorescent polymer light-emitting diodes based on conjugated and non-conjugated

polymers doped with an ir complex. Adv. Mater. **16**, 537–541 (2004). https://doi.org/10.1002/adma.200306331

48. H.J. Kim, C. Lee, M. Godumala, S. Choi, S.Y. Park, M.J. Cho, S. Park, D.H. Choi, Solution-processed thermally activated delayed fluorescence organic light-emitting diodes using a new polymeric emitter containing non-conjugated cyclohexane units. Polym. Chem. **9**, 1318–1326 (2018). https://doi.org/10.1039/c7py02113e
49. M.Y. Wong, Recent advances in polymer organic light-emitting diodes (PLED) using non-conjugated polymers as the emitting layer and contrasting them with conjugated counterparts. J. Electron. Mater. **46**, 6246–6281 (2017). https://doi.org/10.1007/s11664-017-5702-7
50. H. Bronstein, C.B. Nielsen, B.C. Schroeder, I. McCulloch, The role of chemical design in the performance of organic semiconductors. Nat. Rev. Chem. **4**, 66–77 (2020). https://doi.org/10.1038/s41570-019-0152-9
51. N. Thejokalyani, S.J. Dhoble, Novel approaches for energy efficient solid state lighting by RGB organic light emitting diodes—a review. Renew. Sustain. Energy Rev. **32**, 448–467 (2014). https://doi.org/10.1016/j.rser.2014.01.013
52. W. Jiang, X. Ban, M. Ye, Y. Sun, L. Duan, Y. Qiu, A high triplet energy small molecule based thermally cross-linkable hole-transporting material for solution-processed multilayer blue electrophosphorescent devices. J. Mater. Chem. C **3**, 243–246 (2015). https://doi.org/10.1039/C4TC02485K
53. D. de Azevedo, J.N. Freitas, R.A. Domingues, M.M. Faleiros, T.D.Z. Atvars, Correlation between the PL and EL emissions of polyfluorene-based diodes using bilayers or polymer blends. Synth. Met. **233**, 28–34 (2017). https://doi.org/10.1016/j.synthmet.2017.08.015
54. Y. Ma, Z. Zhong, F. Peng, L. Ying, J. Xiong, J. Peng, Y. Cao, Dual hole transport layers for blue-light-emitting PLED: suppress the formation of exciplex towards high device performance and color purity. Org. Electron. **68**, 103–107 (2019). https://doi.org/10.1016/j.orgel.2019.02.008
55. D. Abbaszadeh, P.W.M. Blom, Efficient blue polymer light-emitting diodes with electron-dominated transport due to trap dilution. Adv. Electron. Mater. **2**, 1500406 (2016). https://doi.org/10.1002/aelm.201500406
56. J.C. Germino, J.N. de Freitas, R.A. Domingues, F.J. Quites, M.M. Faleiros, T.D.Z. Atvars, Organic light-emitting diodes based on PVK and Zn(II) salicylidene composites. Synth. Met. **241**, 7–16 (2018). https://doi.org/10.1016/j.synthmet.2018.03.020
57. K.P.S. Zanoni, N.Y. Murakami Iha, Sky-blue OLED through PVK:[Ir(Fppy)2(Mepic)] active layer. Synth. Met. **222**, 393–396 (2016). https://doi.org/10.1016/j.synthmet.2016.11.006
58. K.P.S. Zanoni, A. Ito, N.Y. Murakami Iha, Molecular-engineered [Ir(Fppy) 2 (Mepic)] towards efficient blue-emission. New J. Chem. **39**, 6367–6376 (2015). https://doi.org/10.1039/C5NJ01352F
59. S.K. Mizoguchi, A.O.T. Patrocínio, N.Y. Murakami Iha, On the energy transfer from a polymer host to the rhenium(I) complex in OLEDs. Synth. Met. **159**, 2315–2317 (2009). https://doi.org/10.1016/j.synthmet.2009.08.046
60. A.J. Campbell, D.D.C. Bradley, T. Virgili, D.G. Lidzey, H. Antoniadis, Improving efficiency by balancing carrier transport in poly(9,9-dioctylfluorene) light-emitting diodes using tetraphenylporphyrin as a hole-trapping, emissive dopant. Appl. Phys. Lett. **79**, 3872–3874 (2001). https://doi.org/10.1063/1.1421415
61. C. Li, Y. Wang, D. Sun, H. Li, X. Sun, D. Ma, Z. Ren, S. Yan, Thermally activated delayed fluorescence pendant copolymers with electron- and hole-transporting spacers. ACS Appl. Mater. Interfaces. **10**, 5731–5739 (2018). https://doi.org/10.1021/acsami.8b00136
62. S.M. Ahmad, Elaboration and thermal annealing of the optical properties of the thin films of meta-PPV copolymer. Polym. Bull. **76**, 5345–5362 (2019). https://doi.org/10.1007/s00289-018-2655-9
63. M.R. Andersson, G. Yu, A.J. Heeger, Photoluminescence and electroluminescence of films from soluble PPV-polymers. Synth. Met. **85**, 1275–1276 (1997). https://doi.org/10.1016/S0379-6779(97)80238-X
64. N. Zaquen, L. Lutsen, D. Vanderzande, T. Junkers, Controlled/living polymerization towards functional poly(p-phenylene vinylene) materials. Polym. Chem. **7**, 1355–1367 (2016). https://doi.org/10.1039/C5PY01987G
65. B.J. Lidster, D.R. Kumar, A.M. Spring, C.-Y. Yu, M.L. Turner, Alkyl substituted poly(p-phenylene vinylene)s by ring opening metathesis polymerisation. Polym. Chem. **7**, 5544–5551 (2016). https://doi.org/10.1039/C6PY01186A
66. T. Granier, E.L. Thomas, D.R. Gagnon, F.E. Karasz, R.W. Lenz, Structure investigation of poly(p-phenylene vinylene). J. Polym. Sci. Part B **24**, 2793–2804 (1986). https://doi.org/10.1002/polb.1986.090241214
67. N. Thejo Kalyani, S.J. Dhoble, Organic light emitting diodes: Energy saving lighting technology—a review. Renew. Sustain. Energy Rev. **16**, 2696–2723 (2012). https://doi.org/10.1016/j.rser.2012.02.021
68. J.-H. Kwon, R. Pode, High efficiency red phosphorescent organic light-emitting diodes with simple structure, in *Organic light emitting diode-material, process and devices*. (IntechOpen, London, 2011). https://doi.org/10.5772/18521

69. M.V.M. Rao, C.H. Moon, Solution-processed cesium carbonate doped electron transport layer for multilayered polymer light emitting devices. Optoelectron. Adv. Mater. Rapid Commun. **12**, 164–167 (2018)
70. Y.L. Deng, Y.M. Xie, L. Zhang, Z.K. Wang, L.S. Liao, An efficient organic-inorganic hybrid hole injection layer for organic light-emitting diodes by aqueous solution doping. J. Mater. Chem. C **3**, 6218–6223 (2015). https://doi.org/10.1039/c5tc00851d
71. M. Shan, H. Jiang, Y. Guan, D. Sun, Y. Wang, J. Hua, J. Wang, Enhanced hole injection in organic light-emitting diodes utilizing a copper iodide-doped hole injection layer. RSC Adv. **7**, 13584–13589 (2017). https://doi.org/10.1039/c6ra28644e
72. D. Moghe, D. Kabra, *Polymer Light-Emitting Diodes* (Elsevier Inc., Amsterdam, 2019) https://doi.org/10.1016/B978-0-12-813647-8.00009-6
73. R. Mac Ciarnain, D. Michaelis, T. Wehlus, A.F. Rausch, N. Danz, A. Bräuer, A. Tünnermann, Emission from outside of the emission layer in state-of-the-art phosphorescent organic light-emitting diodes. Org. Electron. **44**, 115–119 (2017). https://doi.org/10.1016/j.orgel.2017.02.006
74. S.L. Lai, S.L. Tao, M.Y. Chan, T.W. Ng, M.F. Lo, C.S. Lee, X.H. Zhang, S.T. Lee, Efficient white organic light-emitting devices based on phosphorescent iridium complexes. Org. Electron. **11**, 1511–1515 (2010). https://doi.org/10.1016/j.orgel.2010.06.011
75. Z. Liu, Z. Bian, F. Hao, D. Nie, F. Ding, Z. Chen, C. Huang, Highly efficient, orange–red organic light-emitting diodes using a series of green-emission iridium complexes as hosts. Org. Electron. **10**, 247–255 (2009). https://doi.org/10.1016/j.orgel.2008.11.013
76. C. Tengstedt, A. Crispin, C. Hsu, C. Zhang, I. Parker, W. Salaneck, M. Fahlman, Study and comparison of conducting polymer hole injection layers in light emitting devices. Org. Electron. **6**, 21–33 (2005). https://doi.org/10.1016/j.orgel.2005.02.001
77. C. Zhang, X. Qiao, Z. Yang, H. Zhang, D. Ma, Highly efficient inverted organic light-emitting diodes with organic p-n junction as electron injection layer. Org. Electron. **58**, 185–190 (2018). https://doi.org/10.1016/j.orgel.2018.03.047
78. Y. Liu, C. Li, Z. Ren, S. Yan, M.R. Bryce, All-organic thermally activated delayed fluorescence materials for organic light-emitting diodes. Nat. Rev. Mater. (2018). https://doi.org/10.1038/natrevmats.2018.20
79. A.E. Nikolaenko, M. Cass, F. Bourcet, D. Mohamad, M. Roberts, Thermally activated delayed fluorescence in polymers: a new route toward highly efficient solution processable OLEDs. Adv. Mater. **27**, 7236–7240 (2015). https://doi.org/10.1002/adma.201501090
80. U. Shakeel, J. Singh, Study of processes of reverse intersystem crossing (RISC) and thermally activated delayed fluorescence (TADF) in organic light emitting diodes (OLEDs). Org. Electron. **59**, 121–124 (2018). https://doi.org/10.1016/j.orgel.2018.04.035
81. J. Kido, Y. Okamoto, Organo lanthanide metal complexes for electroluminescent materials. Chem. Rev. **102**, 2357–2368 (2002). https://doi.org/10.1021/cr010448y
82. Y. Ma, F. Peng, T. Guo, C. Jiang, Z. Zhong, L. Ying, J. Wang, W. Yang, J. Peng, Y. Cao, Semi-orthogonal solution-processed polyfluorene derivative for multilayer blue polymer light-emitting diodes. Org. Electron. **54**, 133–139 (2018). https://doi.org/10.1016/j.orgel.2017.12.037
83. H. Choi, J.S. Park, E. Jeong, G.H. Kim, B.R. Lee, S.O. Kim, M.H. Song, H.Y. Woo, J.Y. Kim, Combination of titanium oxide and a conjugated polyelectrolyte for high-performance inverted-type organic optoelectronic devices. Adv. Mater. **23**, 2759–2763 (2011). https://doi.org/10.1002/adma.201100266
84. M.S. Weaver, L.A. Michalski, K. Rajan, M.A. Rothman, J.A. Silvernail, J.J. Brown, P.E. Burrows, G.L. Graff, M.E. Gross, P.M. Martin, M. Hall, E. Mast, C. Bonham, W. Bennett, M. Zumhoff, Organic light-emitting devices with extended operating lifetimes on plastic substrates. Appl. Phys. Lett. **81**, 2929–2931 (2002). https://doi.org/10.1063/1.1514831
85. J. Kim, P.K.H. Ho, N.C. Greenham, R.H. Friend, Electroluminescence emission pattern of organic light-emitting diodes: implications for device efficiency calculations. J. Appl. Phys. **88**, 1073 (2010)
86. S. Möller, S.R. Forrest, Improved light out-coupling in organic light emitting diodes employing ordered microlens arrays Improved light out-coupling in organic light emitting diodes employing ordered microlens arrays. J. Appl. Phys. **91**, 3324 (2010). https://doi.org/10.1063/1.1435422
87. A. Keawprajak, W. Koetniyom, P. Piyakulawat, K. Jiramitmongkon, S. Pratontep, U. Asawapirom, Effects of tetramethylene sulfone solvent additives on conductivity of PEDOT:PSS film and performance of polymer photovoltaic cells. Org. Electron. **14**, 402–410 (2013). https://doi.org/10.1016/j.orgel.2012.11.005
88. S.P. Mucur, C. Kök, H. Bilgili, B. Canımkurbey, S. Koyuncu, Conventional and inverted organic light emitting diodes based on bright green emmisive polyfluorene derivatives. Polymer (Guildf). **151**, 101–107 (2018). https://doi.org/10.1016/j.polymer.2018.07.063
89. Z. He, C. Jiang, C. Song, J. Wang, Z. Zhong, G. Xie, J. Wang, J. Peng, Y. Cao, Inverted polymer/quantum-dots

hybrid white light emitting diodes. Thin Solid Films **669**, 34–41 (2019). https://doi.org/10.1016/j.tsf.2018.10.028

90. C. Wu, C. Chen, C. Lin, C. Yang, Advanced organic light-emitting devices for enhancing display performances. J. Disp. Technol. **1**, 248–266 (2005)
91. Y. Luo, T. Yu, L. Nian, L. Liu, F. Huang, Z. Xie, Y. Ma, Photoconductive cathode interlayer for enhanced electron injection in inverted polymer light-emitting diodes. ACS Appl. Mater. Interfaces **10**, 11377–11381 (2018). https://doi.org/10.1021/acsami.8b01758
92. Y. Im, M. Kim, Y.J. Cho, J.A. Seo, K.S. Yook, J.Y. Lee, Molecular design strategy of organic thermally activated delayed fluorescence emitters. Chem. Mater. **29**, 1946–1963 (2017). https://doi.org/10.1021/acs.chemmater.6b05324
93. M.Y. Wong, E. Zysman-Colman, Purely organic thermally activated delayed fluorescence materials for organic light-emitting diodes. Adv. Mater. (2017). https://doi.org/10.1002/adma.201605444
94. J. Singh, Radiative recombination and lifetime of a triplet excitation mediated by spin-orbit coupling in amorphous semiconductors. Phys. Rev. B **76**, 1–11 (2007). https://doi.org/10.1103/PhysRevB.76.085205
95. H. Uoyama, K. Goushi, K. Shizu, H. Nomura, C. Adachi, Highly efficient organic light-emitting diodes from delayed fluorescence. Nature **492**, 234–238 (2012). https://doi.org/10.1038/nature11687
96. M. Furno, T.C. Rosenow, M.C. Gather, B. Lüssem, K. Leo, Analysis of the external and internal quantum efficiency of multi-emitter, white organic light emitting diodes analysis of the external and internal quantum efficiency of multi-emitter, white organic light emitting diodes. Appl. Phys. Lett. (2012). https://doi.org/10.1063/1.4757610
97. C. Sun, Y. Wu, Z. Xu, B. Hu, J. Bai, J. Wang, J. Shen, C. Sun, Enhancement of quantum efficiency of organic light emitting devices by doping magnetic nanoparticles Enhancement of quantum efficiency of organic light emitting devices by doping magnetic nanoparticles. Appl. Phys. Lett. **232110**, 1–4 (2011). https://doi.org/10.1063/1.2746415
98. F.B. Dias, K.N. Bourdakos, V. Jankus, K.C. Moss, K.T. Kamtekar, V. Bhalla, J. Santos, M.R. Bryce, A.P. Monkman, Triplet harvesting with 100% efficiency by way of thermally activated delayed fluorescence in charge transfer OLED emitters. Adv. Mater. **25**, 3707–3714 (2013). https://doi.org/10.1002/adma.201300753
99. Z. Ren, R.S. Nobuyasu, F.B. Dias, A.P. Monkman, S. Yan, M.R. Bryce, Pendant homopolymer and copolymers as solution-processable thermally activated delayed fluorescence materials for organic light-emitting diodes. Macromolecules **49**, 5452–5460 (2016). https://doi.org/10.1021/acs.macromol.6b01216
100. G. Xie, J. Luo, M. Huang, T. Chen, K. Wu, S. Gong, C. Yang, Inheriting the characteristics of TADF small molecule by side-chain engineering strategy to enable bluish-green polymers with high PLQYs up to 74% and external quantum efficiency over 16% in light-emitting diodes. Adv. Mater. (2017). https://doi.org/10.1002/adma.201604223
101. S.Y. Lee, T. Yasuda, H. Komiyama, J. Lee, C. Adachi, Thermally activated delayed fluorescence polymers for efficient solution-processed organic light-emitting diodes. Adv. Mater. **28**, 4019–4024 (2016). https://doi.org/10.1002/adma.201505026
102. R.S. Nobuyasu, Z. Ren, G.C. Griffiths, A.S. Batsanov, P. Data, S. Yan, A.P. Monkman, M.R. Bryce, F.B. Dias, Rational design of TADF polymers using a donor-acceptor monomer with enhanced TADF efficiency induced by the energy alignment of charge transfer and local triplet excited states. Adv. Opt. Mater. **4**, 597–607 (2016). https://doi.org/10.1002/adom.201500689
103. Y. Zhu, Y. Zhang, B. Yao, Y. Wang, Z. Zhang, H. Zhan, B. Zhang, Z. Xie, Y. Wang, Y. Cheng, Synthesis and electroluminescence of a conjugated polymer with thermally activated delayed fluorescence. Macromolecules **49**, 4373–4377 (2016). https://doi.org/10.1021/acs.macromol.6b00430
104. Q. Wei, P. Kleine, Y. Karpov, X. Qiu, H. Komber, K. Sahre, A. Kiriy, R. Lygaitis, S. Lenk, S. Reineke, B. Voit, Conjugation-induced thermally activated delayed fluorescence (TADF): from conventional non-TADF units to TADF-active polymers. Adv. Funct. Mater. (2017). https://doi.org/10.1002/adfm.201605051
105. C. Xue, H. Lin, G. Zhang, Y. Hu, W. Jiang, J. Lang, D. Wang, Recent advances in thermally activated delayed fluorescence for white OLEDs applications. J. Mater. Sci. Mater. Electron. (2020). https://doi.org/10.1007/s10854-020-03060-z
106. Y. Jiang, H. Li, Y. Tao, R. Chen, W. Huang, PROGRESS thermally activated delayed fluorescence polymers and applications in organic. Prog. Chem. **31**, 1116 (2019)
107. X. Zeng, J. Luo, T. Zhou, T. Chen, X. Zhou, K. Wu, Y. Zou, G. Xie, S. Gong, C. Yang, Using ring-opening metathesis polymerization of norbornene to construct thermally activated delayed fluorescence polymers: high-efficiency blue polymer light-emitting diodes. Macromolecules **51**, 1598–1604 (2018). https://doi.org/10.1021/acs.macromol.7b02629
108. X. Zhou, M. Huang, X. Zeng, C. Zhong, G. Xie, X. Cao, C. Yang, C. Yang, Superacid-catalyzed Friedel-Crafts polyhydroxyalkylation: a straightforward method to construct

sky-blue thermally activated delayed fluorescence polymers. Polym. Chem. **11**, 3481–3487 (2020). https://doi.org/10.1039/d0py00469c

109. Y. Yang, S. Wang, Y. Zhu, Y. Wang, H. Zhan, Y. Cheng, Thermally activated delayed fluorescence conjugated polymers with backbone-donor/pendant-acceptor architecture for nondoped OLEDs with high external quantum efficiency and low roll-off. Adv. Funct. Mater. **28**, 1–6 (2018). https://doi.org/10.1002/adfm.201706916
110. X. Zhou, M. Huang, X. Zeng, T. Chen, G. Xie, X. Yin, C. Yang, Combining the qualities of carbazole and tetraphenyl silane in a desirable main chain for thermally activated delayed fluorescence polymers. Polym. Chem. **10**, 4201–4208 (2019). https://doi.org/10.1039/c9py00742c
111. L. Wang, X. Cai, B. Bin Li, M. Li, Z. Wang, L. Gan, Z. Qiao, W. Xie, Q. Liang, N. Zheng, K. Liu, S.J. Su, Achieving enhanced thermally activated delayed fluorescence rates and shortened exciton lifetimes by constructing intramolecular hydrogen bonding channels. ACS Appl. Mater. Interfaces (2019). https://doi.org/10.1021/acsami.9b16073
112. C. Li, Y. Xu, Y. Liu, Z. Ren, Y. Ma, S. Yan, Highly efficient white-emitting thermally activated delayed fluorescence polymers: Synthesis, non-doped white OLEDs and electroluminescent mechanism. Nano Energy (2019). https://doi.org/10.1016/j.nanoen.2019.104057
113. J. Rao, X. Liu, X. Li, L. Yang, L. Zhao, S. Wang, J. Ding, L. Wang, Bridging small molecules to conjugated polymers: efficient thermally activated delayed fluorescence with a methyl-substituted phenylene linker. Angew. Chemie - Int. Ed. **59**, 1320–1326 (2020). https://doi.org/10.1002/anie.201912556
114. Y. Wang, Y. Zhu, G. Xie, H. Zhan, C. Yang, Y. Cheng, Bright white electroluminescence from a single polymer containing a thermally activated delayed fluorescence unit and a solution-processed orange OLED approaching 20% external quantum efficiency. J. Mater. Chem. C **5**, 10715–10720 (2017). https://doi.org/10.1039/c7tc03769d
115. G. Grybauskaite-Kaminskiene, K. Ivaniuk, G. Bagdziunas, P. Turyk, P. Stakhira, G. Baryshnikov, D. Volyniuk, V. Cherpak, B. Minaev, Z. Hotra, H. Ågren, J.V. Grazulevicius, Contribution of TADF and exciplex emission for efficient "warm-white" OLEDs. J. Mater. Chem. C **6**, 1543–1550 (2018). https://doi.org/10.1039/c7tc05392d
116. C. Li, J. Liang, B. Liang, Z. Li, Z. Cheng, G. Yang, Y. Wang, An organic emitter displaying dual emissions and efficient delayed fluorescence white OLEDs. Adv. Opt. Mater. **7**, 1–7 (2019). https://doi.org/10.1002/adom.201801667
117. X. Ban, F. Chen, Y. Liu, J. Pan, A. Zhu, W. Jiang, Y. Sun, Design of efficient thermally activated delayed fluorescence blue host for high performance solution-processed hybrid white organic light emitting diodes. Chem. Sci. **10**, 3054–3064 (2019). https://doi.org/10.1039/c8sc05456h
118. Y. Kubo, R. Nishiyabu, White-light emissive materials based on dynamic polymerization in supramolecular chemistry. Polymer (Guildf). **128**, 257–275 (2017). https://doi.org/10.1016/j.polymer.2016.12.082
119. M. Wehner, F. Würthner, Supramolecular polymerization through kinetic pathway control and living chain growth. Nat. Rev. Chem. **4**, 38–53 (2020). https://doi.org/10.1038/s41570-019-0153-8
120. T.F.A. De Greef, M.M.J. Smulders, M. Wolffs, A.P.H.J. Schenning, R.P. Sijbesma, E.W. Meijer, Supramolecular polymerization. Chem. Rev. **109**, 5687–5754 (2009). https://doi.org/10.1021/cr900181u
121. Z. Yin, G. Song, Y. Jiao, P. Zheng, J.-F. Xu, X. Zhang, Dissipative supramolecular polymerization powered by light. CCS Chem **1**, 335–342 (2019). https://doi.org/10.31635/ccschem.019.20190013
122. A. Wild, A. Teichler, C.L. Ho, X.Z. Wang, H. Zhan, F. Schlütter, A. Winter, M.D. Hager, W.Y. Wong, U.S. Schubert, Formation of dynamic metallo-copolymers by inkjet printing: towards white-emitting materials. J. Mater. Chem. C **1**, 1812–1822 (2013). https://doi.org/10.1039/c2tc00552b
123. C.K. Gan, A.F. Sapar, Y.C. Mun, K.E. Chong, Techno-economic analysis of LED lighting: a case study in UTeM's faculty building. Proced. Eng. **53**, 208–216 (2013). https://doi.org/10.1016/j.proeng.2013.02.028
124. J.-C. Su, S.-C. Chou, Performance comparison of polarized white light emitting diodes using wire-grid polarizers with polymeric and glass substrates. Opt. Laser Technol. **100**, 40–44 (2018). https://doi.org/10.1016/j.optlastec.2017.09.041
125. N. Ide, H. Tsuji, N. Ito, H. Sasaki, T. Nishimori, Y. Kuzuoka, K. Fujihara, T. Miyai, T. Komoda, High-performance OLEDs and their application to lighting, in *Organic light emitting materials and devices*. ed. by F. So, C. Adachi (International Society for Optics and Photonics, Bellingham, 2008), p. 705119. https://doi.org/10.1117/12.798190
126. G. Schwartz, S. Reineke, T.C. Rosenow, K. Walzer, K. Leo, Triplet harvesting in hybrid white organic light-emitting diodes. Adv. Funct. Mater. **19**, 1319–1333 (2009). https://doi.org/10.1002/adfm.200801503
127. T.-H. Han, Y. Lee, M.-R. Choi, S.-H. Woo, S.-H. Bae, B.H. Hong, J.-H. Ahn, T.-W. Lee, Extremely efficient flexible organic light-emitting diodes with modified graphene

anode. Nat. Photonics **6**, 105–110 (2012). https://doi.org/10.1038/nphoton.2011.318

128. Y. Zhang, G. Cheng, Y. Zhao, J. Hou, S. Liu, White organic light-emitting devices based on 4,4′-bis(2,2′-diphenyl vinyl)-1,1′-biphenyl and phosphorescence sensitized 5,6,11,12-tetraphenylnaphthacene. Appl. Phys. Lett. **86**, 011112 (2005). https://doi.org/10.1063/1.1845593
129. Y. Yu, W. Lin, X. Peng, Z. Wu, Y. Jin, X. Li, X. Zhang, H. Yang, G. Xie, Realizing an efficient warm white organic light-emitting device possessing excellent color-stability and color rendering index. Org. Electron. **68**, 129–134 (2019). https://doi.org/10.1016/j.orgel.2019.01.037
130. X. Li, J. Cui, Q. Ba, Z. Zhang, S. Chen, G. Yin, Y. Wang, B. Li, G. Xiang, K.S. Kim, H. Xu, Z. Zhang, H. Wang, Multiphotoluminescence from a triphenylamine derivative and its application in white organic light-emitting diodes based on a single emissive layer. Adv. Mater. **31**, 1900613 (2019). https://doi.org/10.1002/adma.201900613
131. H. He, X. Liao, J. Cheng, Y. Li, J. Yu, L. Li, Investigation of energy transfer in star-shaped white polymer light-emitting devices via the time-resolved photoluminescence. Materials (Basel) **11**, 1719 (2018). https://doi.org/10.3390/ma11091719
132. D. Li, W. Hu, J. Wang, Q. Zhang, X.M. Cao, X. Ma, H. Tian, White-light emission from a single organic compound with unique self-folded conformation and multistimuli responsiveness. Chem. Sci. **9**, 5709–5715 (2018). https://doi.org/10.1039/C8SC01915K
133. S. Reineke, M. Thomschke, B. Lüssem, K. Leo, D. Li, W. Hu, J. Wang, Q. Zhang, X.M. Cao, X. Ma, H. Tian, White organic light-emitting diodes: status and perspective. Rev. Mod. Phys. **85**, 1245–1293 (2013). https://doi.org/10.1103/RevModPhys.85.1245
134. J. Liang, L. Ying, F. Huang, Y. Cao, Recent advances in high performance solution processed WOLEDs for solid-state lighting. J. Mater. Chem. C **4**, 10993–11006 (2016). https://doi.org/10.1039/c6tc03468c
135. J. Xu, L. Yu, Z. Sun, T. Li, H. Chen, W. Yang, Efficient, stable and high color rendering index white polymer light-emitting diodes by restraining the electron trapping. Org. Electron. **84**, 105785 (2020). https://doi.org/10.1016/j.orgel.2020.105785
136. B.W. D'Andrade, S.R. Forrest, White organic light-emitting devices for solid-state lighting. Adv. Mater. **16**, 1585–1595 (2004). https://doi.org/10.1002/adma.200400684
137. T.C. Rosenow, M. Furno, S. Reineke, S. Olthof, B. Lüssem, K. Leo, Highly efficient white organic light-emitting diodes based on fluorescent blue emitters. J. Appl. Phys. **108**, 113113 (2010). https://doi.org/10.1063/1.3516481
138. S. Krotkus, D. Kasemann, S. Lenk, K. Leo, S. Reineke, Adjustable white-light emission from a photo-structured micro-OLED array. Light Sci. Appl. **5**, e16121–e16121 (2016). https://doi.org/10.1038/lsa.2016.121
139. P.-A. Will, S. Reineke, Organic light-emitting diodes, in *Handb*. (Org. Mater. Electron. Photonic Devices, Elsevier, Amsterdam, 2019), pp. 695–726. https://doi.org/10.1016/B978-0-08-102284-9.00021-8
140. X. Yang, G. Zhou, W.-Y. Wong, Recent design tactics for high performance white polymer light-emitting diodes. J. Mater. Chem. C **2**, 1760 (2014). https://doi.org/10.1039/c3tc31953a
141. C.-F. Liu, Y. Jiu, J. Wang, J. Yi, X.-W. Zhang, W.-Y. Lai, W. Huang, Star-shaped single-polymer systems with simultaneous RGB emission: design, synthesis, saturated white electroluminescence, and amplified spontaneous emission. Macromolecules **49**, 2549–2558 (2016). https://doi.org/10.1021/acs.macromol.6b00020
142. J. Zou, J. Liu, H. Wu, W. Yang, J. Peng, Y. Cao, High-efficiency and good color quality white light-emitting devices based on polymer blend. Org. Electron. **10**, 843–848 (2009). https://doi.org/10.1016/j.orgel.2009.04.007
143. X.D. Zhu, Y.L. Zhang, Y. Yuan, Q. Zheng, Y.J. Yu, Y. Li, Z.Q. Jiang, L.S. Liao, Incorporating a tercarbazole donor in a spiro-type host material for efficient RGB phosphorescent organic light-emitting diodes. J. Mater. Chem. C **7**, 6714–6720 (2019). https://doi.org/10.1039/c9tc01426h
144. M. Yin, T. Pan, Z. Yu, X. Peng, X. Zhang, W. Xie, S. Liu, L. Zhang, Color-stable WRGB emission from blue OLEDs with quantum dots-based patterned down-conversion layer. Org. Electron. **62**, 407–411 (2018). https://doi.org/10.1016/j.orgel.2018.08.036
145. C. Zhao, T. Schwartz, B. Stöger, F.J. White, J. Chen, D. Ma, J. Fröhlich, P. Kautny, Controlling excimer formation in indolo[3,2,1-jk] carbazole/9 H -carbazole based host materials for RGB PhOLEDs. J. Mater. Chem. C **6**, 9914–9924 (2018). https://doi.org/10.1039/c8tc03537g
146. W. Wu, M. Inbasekaran, M. Hudack, D. Welsh, W. Yu, Y. Cheng, C. Wang, S. Kram, M. Tacey, M. Bernius, R. Fletcher, K. Kiszka, S. Munger, J. O'Brien, Recent development of polyfluorene-based RGB materials for light emitting diodes. Microelectron. J. **35**, 343–348 (2004). https://doi.org/10.1016/j.mejo.2003.07.001
147. L. Bai, B. Liu, Y. Han, M. Yu, J. Wang, X. Zhang, C. Ou, J. Lin, W. Zhu, L. Xie, C. Yin, J. Zhao, J. Wang, D.D.C. Bradley, W. Huang, Steric-hindrance-functionalized polydiarylfluorenes: conformational behavior, stabilized blue electroluminescence, and efficient amplified spontaneous

emission. ACS Appl. Mater. Interfaces **9**, 37856–37863 (2017). https://doi.org/10.1021/acsami.7b08980

148. D.A. Moghe, A. Dey, K. Johnson, L.-P. Lu, R.H. Friend, D. Kabra, Ultrafast endothermic transfer of non-radiative exciplex state to radiative excitons in polyfluorene random copolymer for blue electroluminescence. Appl. Phys. Lett. **112**, 163301 (2018). https://doi.org/10.1063/1.5020928
149. X. Zhang, Q. Hu, J. Lin, Z. Lei, X. Guo, L. Xie, W. Lai, W. Huang, Efficient and stable deep blue polymer light-emitting devices based on β -phase poly(9,9-dioctylfluorene). Appl. Phys. Lett. **103**, 153301 (2013). https://doi.org/10.1063/1.4824766
150. P. Petrova, R. Tomova, ChemInform abstract: materials used for organic light-emitting diodes: organic electroactive compounds. ChemInform. (2010). https://doi.org/10.1002/chin.201026253
151. S. Beaupré, M. Leclerc, I. Lévesque, M. D'Iorio, Design, synthesis and charaterization of polymers derived from fluorene for application in rgb polymer light-emitting-diodes. MRS Proc. (2001). https://doi.org/10.1557/PROC-665-C5.34
152. J. Liu, J. Zou, W. Yang, H. Wu, C. Li, B. Zhang, J. Peng, Y. Cao, Highly efficient and spectrally stable blue-light-emitting polyfluorenes containing a dibenzothiophene- S, S -dioxide unit. Chem. Mater. **20**, 4499–4506 (2008). https://doi.org/10.1021/cm800129h
153. F. Peng, Z. Zhong, Y. Ma, Z. Huang, L. Ying, J. Xiong, S. Wang, X. Li, J. Peng, Y. Cao, Achieving highly efficient blue light-emitting polymers by incorporating a styry-larylene amine unit. J. Mater. Chem. C **6**, 12355–12363 (2018). https://doi.org/10.1039/C8TC04411B
154. J.H. Lee, C.H. Chen, P.H. Lee, H.Y. Lin, M.K. Leung, T.L. Chiu, C.F. Lin, Blue organic light-emitting diodes: current status, challenges, and future outlook. J. Mater. Chem. C **7**, 5874–5888 (2019). https://doi.org/10.1039/c9tc00204a
155. V.N. Bliznyuk, S.A. Carter, J.C. Scott, G. Klärner, R.D. Miller, D.C. Miller, Electrical and photoinduced degradation of polyfluorene based films and light-emitting devices. Macromolecules **32**, 361–369 (1999). https://doi.org/10.1021/ma9808979
156. L. Romaner, A. Pogantsch, P. Scandiucci de Freitas, U. Scherf, M. Gaal, E. Zojer, E.J.W. List, The origin of green emission in polyfluorene-based conjugated polymers: on-chain defect fluorescence. Adv. Funct. Mater. **13**, 597–601 (2003). https://doi.org/10.1002/adfm.200304360
157. J.M. Lupton, J. Klein, Time-gated electroluminescence spectroscopy of polymer light-emitting diodes as a probe of carrier dynamics and trapping. Phys. Rev. B **65**, 193202 (2002). https://doi.org/10.1103/PhysRevB.65.193202
158. E. Zojer, A. Pogantsch, E. Hennebicq, D. Beljonne, J.-L. Brédas, P. Scandiucci de Freitas, U. Scherf, E.J.W. List, Green emission from poly(fluorene)s: the role of oxidation. J. Chem. Phys. **117**, 6794–6802 (2002). https://doi.org/10.1063/1.1507106
159. A.P. Kulkarni, X. Kong, S.A. Jenekhe, Fluorenone-containing polyfluorenes and oligofluorenes: photophysics, origin of the green emission and efficient green electroluminescence. J. Phys. Chem. B **108**, 8689–8701 (2004). https://doi.org/10.1021/jp037131h
160. D. Kabra, M.H. Song, B. Wenger, R.H. Friend, H.J. Snaith, High efficiency composite metal oxide-polymer electroluminescent devices: a morphological and material based investigation. Adv. Mater. **20**, 3447–3452 (2008). https://doi.org/10.1002/adma.200800202
161. A.R. Davis, K.R. Carter, Controlling optoelectronic behavior in poly(fluorene) networks using thiol-ene photoclick chemistry. Macromolecules **48**, 1711–1722 (2015). https://doi.org/10.1021/ma5014226
162. F. Baycan Koyuncu, A.R. Davis, K.R. Carter, Emissive conjugated polymer networks with tunable band-gaps via thiol-ene click chemistry. Chem. Mater. **24**, 4410–4416 (2012). https://doi.org/10.1021/cm302790a
163. C.L. Donley, J. Zaumseil, J.W. Andreasen, M.M. Nielsen, H. Sirringhaus, R.H. Friend, J.-S. Kim, Effects of packing structure on the optoelectronic and charge transport properties in poly(9,9-di- n -octylfluorene- alt -benzothiadiazole). J. Am. Chem. Soc. **127**, 12890–12899 (2005). https://doi.org/10.1021/ja051891j
164. F.A. Feist, M.F. Zickler, T. Basché, Origin of the red sites and energy transfer rates in single MEH-PPV chains at low temperature. ChemPhysChem **12**, 1499–1508 (2011). https://doi.org/10.1002/cphc.201001010
165. B.R. Lee, W. Lee, T.L. Nguyen, J.S. Park, J.-S. Kim, J.Y. Kim, H.Y. Woo, M.H. Song, Highly efficient red-emitting hybrid polymer light-emitting diodes via förster resonance energy transfer based on homogeneous polymer blends with the same polyfluorene backbone. ACS Appl. Mater. Interfaces **5**, 5690–5695 (2013). https://doi.org/10.1021/am401090m
166. Z. Liu, L. Zhang, X. Gao, Q. Zhang, S. Shi, Synthesis and characterization of novel red-emitting conjugated polymers based on triphenylaminesilole-carbazole-fluorene. Mater. Chem. Phys. **212**, 208–213 (2018). https://doi.org/10.1016/j.matchemphys.2018.01.060
167. Q. Hou, Q. Zhou, Y. Zhang, W. Yang, R. Yang, Y. Cao, Synthesis and electroluminescent properties of high-efficiency saturated red emitter based on copolymers from fluorene and 4,7-di(4-hexylthien-2-yl)-2,1,3-

benzothiadiazole. Macromolecules **37**, 6299–6305 (2004). https://doi.org/10.1021/ma049204g

168. X.Y. Shang, S.J. Wang, X.C. Ge, M. Xiao, Y.Z. Meng, Synthesis and photoluminescent properties of poly(arylene ether)s containing oxadiazole and fluorene moieties. Mater. Chem. Phys. **104**, 215–219 (2007). https://doi.org/10.1016/j.matchemphys.2007.02.049
169. L. Chen, B. Zhang, Y. Cheng, Z. Xie, L. Wang, X. Jing, F. Wang, Pure and saturated red electroluminescent polyfluorenes with dopant/host system and PLED efficiency/color purity trade-offs. Adv. Funct. Mater. **20**, 3143–3153 (2010). https://doi.org/10.1002/adfm.201000840
170. J. Zaumseil, C.R. McNeill, M. Bird, D.L. Smith, P. Paul Ruden, M. Roberts, M.J. McKiernan, R.H. Friend, H. Sirringhaus, Quantum efficiency of ambipolar light-emitting polymer field-effect transistors. J. Appl. Phys. **103**, 064517 (2008). https://doi.org/10.1063/1.2894723
171. U. Scherf, E.J.W. List, Semiconducting polyfluorenes—towards reliable structure-property relationships. Adv. Mater. **14**, 477–487 (2002). https://doi.org/10.1002/1521-4095(20020404)14:7%3c477::AID-ADMA477%3e3.0.CO;2-9
172. X. Gao, Y. Zhang, C. Fang, X. Cai, B. Hu, G. Tu, Efficient deep-red electroluminescent donor-acceptor copolymers based on 6,7-dichloroquinoxaline. Org. Electron. **46**, 276–282 (2017). https://doi.org/10.1016/j.orgel.2017.04.002
173. K.M. Nimith, M.N. Satyanarayan, G. Umesh, Enhancement in fluorescence quantum yield of MEH-PPV:BT blends for polymer light emitting diode applications. Opt. Mater. (Amst) **80**, 143–148 (2018). https://doi.org/10.1016/j.optmat.2018.04.046
174. J.H. Kim, J.H. Yun, J.Y. Lee, Recent progress of highly efficient red and near-infrared thermally activated delayed fluorescent emitters. Adv. Opt. Mater. **6**, 1–16 (2018). https://doi.org/10.1002/adom.201800255
175. J. Li, T. Nakagawa, J. Macdonald, Q. Zhang, H. Nomura, H. Miyazaki, C. Adachi, Highly efficient organic light-emitting diode based on a hidden thermally activated delayed fluorescence channel in a heptazine derivative. Adv. Mater. **25**, 3319–3323 (2013). https://doi.org/10.1002/adma.201300575
176. W. Zeng, H.Y. Lai, W.K. Lee, M. Jiao, Y.J. Shiu, C. Zhong, S. Gong, T. Zhou, G. Xie, M. Sarma, K.T. Wong, C.C. Wu, C. Yang, Achieving nearly 30% external quantum efficiency for orange-red organic light emitting diodes by employing thermally activated delayed fluorescence emitters composed of 1,8-naphthalimide-acridine hybrids. Adv. Mater. **30**, 1–8 (2018). https://doi.org/10.1002/adma.201704961
177. Q. Zhao, J.Z. Sun, Red and near infrared emission materials with AIE characteristics. J. Mater. Chem. C **4**, 10588–10609 (2016). https://doi.org/10.1039/c6tc03359h
178. T. Sudyoadsuk, P. Chasing, C. Chaiwai, T. Chawanpunyawat, T. Kaewpuang, T. Manyum, S. Namuangruk, V. Promarak, Highly fluorescent solid-state benzothiadiazole derivatives as saturated red emitters for efficient solution-processed non-doped electroluminescent devices. J. Mater. Chem. C **8**, 10464–10473 (2020). https://doi.org/10.1039/d0tc02131h
179. K. Imamori, A. Masuda, H. Matsumura, Influence of a-Si:H deposition by catalytic CVD on transparent conducting oxides. Thin Solid Films **395**, 147–151 (2001). https://doi.org/10.1016/S0040-6090(01)01241-X
180. Y.-C. Wang, H.-N. Chen, W.-Y. Li, M.-C. Chan, Non-invasive biopsy of doped-ions inside optical substrate by modified two-photon microscopy. Opt. Express **23**, 1871 (2015). https://doi.org/10.1364/oe.23.001871
181. I.S. Song, S.W. Heo, J.H. Lee, J.R. Haw, D.K. Moon, Study on the wet processable antimony tin oxide (ATO) transparent electrode for PLEDs. J. Ind. Eng. Chem. **18**, 312–316 (2012). https://doi.org/10.1016/j.jiec.2011.11.051
182. K.L. Chopra, S. Major, D.K. Pandya, Transparent conductors-a status review. Thin Solid Films **102**, 1–46 (1983). https://doi.org/10.1016/0040-6090(83)90256-0
183. Z. Yu, Q. Zhang, L. Li, Q. Chen, X. Niu, J. Liu, Q. Pei, Highly flexible silver nanowire electrodes for shape-memory polymer light-emitting diodes. Adv. Mater. **23**, 664–668 (2011). https://doi.org/10.1002/adma.201003398